FILM COOLING FOLLOWING INJECTION THROUGH INCLINED CIRCULAR TUBES

R. J. Goldstein
E. R. G. Eckert
V. L. Eriksen
J. W. Ramsey

prepared for

NATIONAL AERONAUTICS AND SPACE ADMINISTRATION

NASA CONTRACT NO. NAS 3-7904

HEAT TRANSFER LABORATORY

MECHANICAL ENGINEERING DEPARTMENT

UNIVERSITY OF MINNESOTA

Requests for copies of this report should be referred to:

National Aeronautics and Space Administration
Office of Scientific and Technical Information
P.O. Box 33
College Park, Maryland 20740

NASA CR-72612
HTL TR NO. 91

SUMMARY REPORT

FILM COOLING FOLLOWING INJECTION THROUGH INCLINED CIRCULAR TUBES

by

R.J. Goldstein, E.R.G. Eckert,
V.L. Eriksen and J.W. Ramsey

prepared for

NATIONAL AERONAUTICS AND SPACE ADMINISTRATION

November 1969

CONTRACT NAS 3-7904
TECHNICAL MANAGEMENT
NASA Lewis Research Center
Cleveland, Ohio
Lewis Project Manager; Francis S. Stepka

University of Minnesota
Institute of Technology
Department of Mechanical Engineering
Minneapolis, Minnesota 55455

ABSTRACT

Film cooling effectiveness measurements with injection of air through discrete holes into a turbulent boundary layer of air on a flat plate are described. The secondary air is injected through either a single hole or a row of holes spaced at three diameter intervals across the span with an injection angle of 35 degrees to the flow and in a different series of tests through a single hole with lateral injection angles of either 15^{o} or 35^{o}. Results are compared with earlier tests to show that the film cooling effectiveness increases as the boundary layer thickness at the injection location is decreased. Data from single hole tests are similar to that for a row of holes at low blowing rates, but significant differences are observed at higher blowing rates. The effect of lateral injection is to provide cooling over a wider area than when injection is normal to the flow or inclined downstream only.

NOMENCLATURE

D	diameter of injection tube
M	blowing rate parameter, $\rho_2 U_2 / \rho_\infty U_\infty$
S_D	spacing between holes in tube diameters (i.e. $S_D \cdot D$ is linear dimension across span between centerlines of adjacent holes)
T	temperature
T_{aw}	adiabatic wall temperature
T_2	temperature of secondary air
T_∞	mainstream temperature
U	velocity
U_2	average air velocity in injection tube
U_∞	mainstream velocity
X	distance downstream of injection hole, see Figure 1
Y	distance normal to tunnel floor, see Figure 1
Z	lateral distance from injection hole, see Figure 1
β	injection angle with the flow, measured from X axis in the X-Y plane, see Figure 1(a)
δ^*	boundary layer displacement thickness
η	$\eta(x,z)$, local film cooling effectiveness following injection through a single hole or a row of holes, defined by Equation 1
η_1	$\eta_1(x,z)$, local film cooling effectiveness following injection through a single hole

η_r $\eta_r(x,z)$, local film cooling effectiveness following injection through a row of holes

$\bar{\eta}$ $\bar{\eta}(x)$, laterally averaged film cooling effectiveness downstream of a row of holes, defined by Equation 2

$\bar{\eta}_p$ $\bar{\eta}_p(x)$, predicted average film cooling effectiveness across the span for injection through a row of holes using results from single hole injection and the principle of superposition, defined by Equation 4

$\tilde{\eta}$ $\tilde{\eta}(x)$, lateral integral of the film cooling effectiveness produced by injection through a single hole, defined by Equation 3

Φ lateral injection angle, measured from Z axis in the Y-Z plane, see Figure 1(b)

ν_∞ kinematic viscosity of mainstream

ρ density

ρ_2 density of secondary air

ρ_∞ density of mainstream

FILM COOLING FOLLOWING INJECTION THROUGH INCLINED CIRCULAR TUBES

by

R.J. Goldstein, E.R.G. Eckert,

V.L. Eriksen and J.W. Ramsey

University of Minnesota

I. SUMMARY

The study described in this summary report was carried out under NASA Contract NAS 3-7904. It is part of an extended investigation into film cooling following ejection of a secondary gas through discrete holes into a turbulent boundary layer of air on a flat plate. This report presents adiabatic wall temperature measurements downstream of heated jets of air in a subsonic wind tunnel.

Four different injection systems are used--a single tube inclined at an angle of 35^{o} with the flow, a row of tubes at an angle of 35^{o} with the flow and spaced at intervals of three diameters across the span, and single tubes at lateral angles of 35^{o} and 15^{o}. The surface on which the wall temperatures are measured is designed to minimize conduction parallel to its surface in addition to being well insulated in the direction normal to its surface. Thus the temperatures measured approximate local adiabatic wall tem-

peratures. Similar trends are observed as were in a previous study with a larger diameter injection tube. The film cooling effectiveness increases as the dimensionless boundary layer thickness is decreased for this injection system. This trend is attributed to greater turning of the jet due to higher relative velocities near the wall for the thinner boundary layer.

At high blowing rates the film cooling effectiveness is observed to be significantly higher for a row of holes than for single hole injection. The row of jets blocks a greater area of the mainstream than a single jet, resulting in a greater force on the row of jets. The row of jets is then turned more than a single jet, forcing the flow closer to the wall and resulting in higher film cooling effectivenesses. The effect of lateral injection is to widen the temperature field at low blowing rates where the jet remains near the wall and to hold the jet closer to the wall at high blowing rates where the jet would otherwise flow into the mainstream.

II. INTRODUCTION

Film cooling is used extensively to protect structural elements from a hot gas stream. A coolant (only gas is considered in the present study) is ejected locally through the wall of the structure to be protected, isolating the structure from the hot gas stream. Actually instead of having a

discrete film the secondary fluid usually mixes with the boundary layer. The wall is protected by the resulting lower temperature and thicker boundary layer. The coolant can be ejected through a continuous slot, through a strip of porous material, or through an arrangement of discrete openings in single or multiple rows.

Continuous slots or porous strips are an effective arrangement for film cooling injection. However, in certain applications, such as gas turbine blade cooling, stress or manufacturing considerations make it impractical to use continuous slots or porous strips, and rows of discrete openings are preferable. A study of film cooling with such an arrangement is complicated by the three dimensional nature of the flow and temperature fields downstream from the openings, and only sparse information is available for the efficacy of this cooling method [1][2]. Some earlier research has been reported on injection through discrete holes [3][4] and a recent work [5] reports average (over the plate span and length) film cooling effectiveness downstream of a row of holes.

The present paper reports the results of part of an extended investigation into film cooling with ejection of the secondary gas through discrete holes. The initial results of this study, [1][2], dealt with ejection through a single circular hole at angles of 90 and 35 degrees with the flow. Adiabatic wall temperatures were reported as a function of

position with the blowing rate, M, as a parameter. Only a slight variation of Reynolds number, $U_\infty D/\nu_\infty$, was possible. The present paper reports--as a continuation of the study--injection through a hole with smaller diameter at an angle β (see Fig. 1(a)) of 35° with the flow. As in [1] and |2|, adiabatic wall temperature distributions downstream of heated jets of air are investigated. In addition to the effect of blowing parameter, the influence of the turbulent boundary layer displacement thickness at the point of injection is considered. Results are also reported for a row of holes at an angle β of 35 degrees with the flow, and for injection through single holes at angles Φ (see Fig. 1(b)) of 15 and 35 degrees with the lateral directions.

The injection tubes are 1.18 cm in diameter and the temperature of the injected air is approximately 55°C higher than that of the mainstream. The range of variables studied is as follows: freestream velocity of 30.5 to 61.0 m/s, displacement thickness of the turbulent boundary layer at the point of injection from 0.078 cm to 0.146 cm, and blowing parameter (ratio of the mass flux of the injected flow to the mass flux of the mainstream) of 0.1 to 2.0.

III. EXPERIMENTAL APPARATUS

The apparatus used in this study is the same as that described earlier [1] and [2] with a few alterations in the

method of secondary injection. The wind tunnel shown in Figure 2 draws the air mainstream from the room through an entrance section, the test section, a diffuser, a blower, and finally through a silencer before being discharged to the outside.

The secondary or injected air is supplied by the building air compressor. The flow rate is controlled by a needle valve and is measured with a thin plate orifice meter. Temperature fluctuations introduced by the compressor are eliminated by passing the air through a long coiled copper tubing submerged in a large tank of water. The air is heated in a stainless steel tube around which heating tapes are wrapped.

The orientation of the tubes in the injection section is best described with the aid of Figure 1. The multiple hole section contains five tubes spaced laterally across the tunnel at three diameter center to center spacing. These tubes have their outlet in the injection plate which can be moved along the bottom of the tunnel in a direction normal to the tunnel axis. The orientation is similar to that shown in Figure 1(a) with β = 35 degrees. For single hole injection at an angle of 35^{o} with the flow the side holes in this same injection section are covered by tape and only the center hole is used to inject air.

The injection sections for lateral injection have tubes shown in Figure 1(b). The angle β with the flow is equal to 90^{o} in these sections while the lateral angles, Φ, are 15

and 35 degrees, respectively. Each section contains a single tube.

The test section bottom wall is close to being adiabatic. It is well insulated in the direction normal to its surface and is designed to have negligible conduction in all directions parallel to its surface as well, so that local adiabatic temperatures can be measured. Three columns (in the flow direction) of calibrated thermocouples are located in this surface, one along the center of the test section, and one each at distances of 7.5 cm on either side. A detailed description of this wall is contained in references 1 and 2.

IV. TUNNEL OPERATING CONDITIONS

With no secondary injection in the tunnel, the velocity profile at the injection location is flat except for the boundary layers on the walls of the test section. A fully developed turbulent boundary layer profile exists on the test surface. The displacement thickness of this boundary layer varies from 0.078 cm to 0.146 cm at the point of injection for different injection sections and for various tunnel velocities. The mainstream has no swirl and a turbulence intensity of about 0.5%. The tunnel is operated at uniform free stream velocities of 30.5 and 61.0 m/s.

In the absence of a free stream flow in the test section,

a fully developed turbulent velocity profile exists at the end of each injection tube. The temperature profile is quite flat at approximately 55°C above the temperature of the main flow. There is approximately a one percent variation in excess temperature across the five hole injection section, the center tube being at the highest temperature and the outer tubes at the lowest. The temperature difference between the outer tubes and the neighboring tubes is much greater than the difference between the center and the adjacent tubes so that the temperature difference between tubes in the vicinity of the center tube where measurements are taken is much less than one percent. No variation in flow rate can be detected between any of the five tubes.

V. ADIABATIC WALL TEMPERATURE AND AVERAGE LATERAL FILM COOLING EFFECTIVENESS

Adiabatic wall temperatures are presented in the form of a film cooling effectiveness:

$$\eta = \frac{T_{aw} - T_\infty}{T_2 - T_\infty} \tag{1}$$

The adiabatic wall temperature is defined as that temperature which is established in steady state at any location on the insulated surface under the influence of the flow described in the foregoing when heat conduction within the plate and

radiative transfer are absent. It is measured by the thermocouples installed along the centerline of the test plate. By moving the injection section laterally, this row of thermocouples us also used to measure the axial temperature distribution at various lateral positions, Z, from the jet. The mainstream temperature, T_∞, is measured by thermocouples in the test plate at positions unaffected by the injection. The secondary air temperature, T_2, is taken as that measured by the thermocouples attached to the injection tubes 4½ and 6 diameters upstream of their ends. These locations are far enough upstream from the tube exit to be insensitive to temperature distortions caused by the mainstream flow and by the conduction from the tube to the injection plate.

The laterally averaged film cooling effectiveness following injection through a row of holes is

$$\bar{\eta} = \frac{1}{S_D \cdot D} \int_{-\frac{S_D \cdot D}{2}}^{\frac{S_D \cdot D}{2}} \eta_r(x,z)\, dz \qquad (2)$$

where S_D is the hole spacing in tube diameters (i.e. $S_D \cdot D$ is linear distance across span between centerlines of adjacent holes) and $\eta_r(x,z)$ is the film cooling effectiveness distribution for a row of holes. If there were no interaction between the jets along a row then the lateral temperature distribution for a row of holes could be found by the principle of superposition, i.e. summing up the contributions

to the film cooling effectiveness from each individual hole in the row (see Fig. 3). The effect across the span of single hole injection can be defined by

$$\tilde{\eta} = \frac{1}{D} \int_{-\infty}^{\infty} \eta_1(x,z)\, dz \tag{3}$$

where $\eta_1(x,z)$ is the film cooling effectiveness distribution for single hole injection. The predicted average effectiveness for a row of such holes is then

$$\bar{\eta}_p = \frac{\tilde{\eta}}{S_D}$$

$$= \frac{1}{S_D \cdot D} \int_{-\infty}^{\infty} \eta_1(x,z)\, dz \tag{4}$$

Comparison of $\bar{\eta}$ with $\bar{\eta}_p$ gives a measure of how well the method of superposition works. Comparison of values of $\tilde{\eta}$ for different geometries of single hole injection indicates the total cooling effect (across the span) of the jet at a given distance downstream of injection.

VI. EXPERIMENTAL RESULTS

Results of the single hole experiments with injection at an angle of 35^{o} with the flow are shown on Figures 4-11. Figures 4-7 represent runs at a free stream velocity of 30.5 m/s; Figures 8-11 represent runs at 61.0 m/s. These data display the same trends as earlier data [1][2] taken with

injection through a tube which had twice the diameter of the present one. The film cooling effectiveness at any location is highest for the blowing rate M≅0.5. At M=2.0, the effectiveness is very low at all locations, indicating that the jet penetrates into the mainstream and does not remain near the wall. The film cooling effectiveness on the centerline (Z/D=0.0) decreases with X/D while at larger values of Z/D it first increases with X/D before decreasing. This result is attributed to the spreading of the jet.

Figure 12 compares some results from Figures 4-11 for two different values of the freestream velocity at three different blowing rates. The runs at M=0.5 and 1.0 show the effectiveness to be higher for the higher freestream velocity. The effectiveness values at M=2.0 are so small that comparisons between them are meaningless. Since both the Reynolds number and the boundary layer thickness vary with the freestream velocity, it is difficult to decide which parameter causes the differences between the curves for the two velocities on this graph.

The combined effect of both free stream velocity and injection tube diameter at a fixed value of the Reynolds number, $U_\infty D/\nu_\infty$, can be observed in Figure 13. The data for the larger diameter tube are taken from references 1 and 2. The solid symbols, representing the larger diameter tube and lower freestream velocity, show the centerline film cooling effectiveness to be higher than the open symbols that repre-

sent the runs with the smaller diameter tube and higher velocity. This indicates that the boundary layer thickness influences the effectiveness.

Figure 14 shows the centerline film cooling effectiveness at three different downstream locations as a function of the dimensionless boundary layer displacement thickness, δ^*/D. The data on this figure is not all at one value of the Reynolds number, $U_\infty D/\nu_\infty$. The data with the closed points on the left of the graphs are for the larger diameter hole [1][2]; the data with the open points on the right refer to the smaller diameter hole. For each set, the higher velocity run lies to the left of the lower velocity run. The data show a definite trend--the film cooling effectiveness decreases as the dimensionless boundary layer displacement thickness is increased. This trend seems quite reasonable. As the injected air enters the mainstream boundary layer it encounters a higher relative velocity at positions closer to the wall for a thinner boundary layer. This has the effect of turning the injected air more rapidly, decreasing its penetration, and therefore leading to higher values of the film cooling effectiveness.

Data taken with a row (across the span) of injection holes are presented in Figures 15-17. The tubes, which are at an angle of 35^o with the flow, are spaced laterally at three diameter intervals. Some values from Figure 17 are compared with data for a single hole under the same conditions in

Figure 18. At blowing rates of M=0.5 and 1.0, there is little difference between the data for a single hole and for a row of holes. The centerline values are nearly identical and the values midway between holes (Z/D=1.5) are only slightly higher for a row of holes.

If the film cooling effectiveness values for a row of holes is calculated from the superposition of single hole values as in some film cooling models (at low blowing rates) centerline values for a single hole and a row of holes should be nearly identical since the film cooling effectiveness for a single hole at Z/D=3.0 is very small. Superposition also predicts an effectiveness for a row of holes twice as large as for a single hole at Z/D=1.5. Figure 18 shows that the centerline values compare favorably at M=0.5 and approximately at M=1.0, but the data midway between holes (Z/D=1.5) do not follow the expected trend (i.e. they are not significantly larger for the row of holes).

Lateral averages for some of the multiple hole data and predicted lateral averages from single hole data are presented in Figure 19. Also shown is a correlation [6] for the film cooling effectiveness downstream of a two dimensional slot at an angle of 35^{o} for M=0.5. The outlet area of the slot is considered to be the same as the area of the row of holes spaced at three diameter intervals. The mass injection per unit span is thus the same for the row of holes and for the slot at the same blowing rate. For M=0.5 the principle of

superposition predicts slightly higher spanwise average effectiveness for a row of holes than was measured. Both the predicted and the measured average values for the row of holes fall below the value for slot injection. At M=1.0 agreement between superimposed single hole and multiple hole data is quite good for about the first 25 diameters downstream of injection. Further downstream the centerline single hole results continue to decrease while the multiple hole results remain fairly constant.

Differences in the film cooling effectiveness for injection through a single hole and injection through a row of holes appear at higher blowing rates (Fig. 18 and 19). Whereas the single hole results for M=1.5 and 2.0 decrease with X/D to very small values of η, the row of holes data approach a relatively constant value of η. At M=1.5, the centerline film cooling effectiveness of the row of holes remains at approximately 0.1 while the effectiveness midway between holes (Z/D=1.5) increases to this value as the jets spread. The measured $\overline{\eta}$ for a row of holes increases slightly with X/D while $\overline{\eta}_p$ decreases when calculated from measurements for a single hole at M=1.5. At M=2.0, both the centerline and between-hole effectivenesses increase to approximately 0.13 at X/D=20. The increase in effectiveness from the injection location to X/D=20 is probably due to jet spreading toward the wall. The single hole effectiveness at M=2.0 is much smaller (too small to measure at Z/D=1.5 and too small to

evaluate $\tilde{\eta}$ and $\bar{\eta}_p$ accurately). $\bar{\eta}$ for a row of holes at M=2.0 increases to a constant value of approximately 0.13.

These differences between single hole and multiple hole injection can also be observed on Figure 20 where the centerline value of the film cooling effectiveness is cross-plotted against the blowing parameter M at several axial positions. The peak effectiveness for single hole injection is located at a blowing rate of approximately 0.5 as it was in [1]and [2]. The values for multiple hole injection are higher than their counterparts for single hole injection at the higher blowing rates. The increased effectiveness of a row of holes compared to a single hole is attributed to the greater blockage that the main flow faces with the row of jets. There is less area available for the mainstream to flow around and under the row of jets than with a single jet. This is particularly true some distance downstream of injection, resulting in a greater turning of the row of jets forcing the flow down towards the wall. Higher effectiveness is not observed at low blowing rates for a row of holes since the jets do not then significantly depart from the wall.

Figures 21 and 22 present film cooling effectiveness results for injection at lateral angles of 35 and 15 degrees respectively. The film cooling effectiveness is presented as a function of lateral position Z/D with location in the flow direction X/D as a parameter. The projections of the inside edges of the circular tube through which the secondary

fluid is injected are shown on the Z/D axis at ±0.87 for $\Phi=35^{o}$ and ±1.93 for $\Phi=15^{o}$. Values of $\tilde{\eta}$ for injection through these laterally inclined tubes are presented in Figure 23. In these tests the highest values of both the peak effectiveness and the lateral integral of the effectiveness for $\Phi=35^{o}$ occur at M=0.5 near the hole. Downstream the lateral integral becomes slightly larger for M=1.0 as compared to M=0.5. Effectiveness values for M=2.0 are very low, indicating that the jet has penetrated into the main flow. For $\Phi=15^{o}$ the maximum local effectiveness for M=1.0 is slightly higher than for M=0.5, but the wider field of high effectiveness and the larger values of $\tilde{\eta}$ for M=0.5 indicate that this is the more effective blowing rate. The values of $\tilde{\eta}$ are higher for $\Phi=15^{o}$ than for $\Phi=35^{o}$. The jet is expected to remain closer to the wall for the smaller angle resulting in a larger film cooling effectiveness. In general the laterally integrated effectiveness ($\tilde{\eta}$) with lateral injection is higher than for injection through the single hole inclined downstream except far downstream at M=0.5.

To show the effect of normal injection on the total cooling effect of a jet, lateral integrals of data from [1] and [2] are presented in Figure 24. The open symbols are for normal injection, the solid ones are for injection at an angle of 35^{o} with the flow. The solid symbols from this plot differ from the data from Figure 23 for injection at an angle of 35^{o} with the flow because of different values of

free stream velocity and hole diameter (cf. Figure 14). At M=0.5, where the jets remain near the wall, Figure 24 shows that injection at an angle of 35^{o} with the flow yields higher integrated values of the film cooling effectiveness than normal injection does. At M=1.0, where both jets penetrate into the main flow, the integrated values are actually higher for normal injection (possibly due to the greater jet mixing and spreading with normal injection).

Figures 25 and 26 contain contours of constant film cooling effectiveness on the floor of the test section. These curves are determined by an interpolation scheme that fits quadratic equations to sets of three data points. Figure 25 is for data at M=0.5; Figure 26 is for M=1.0. On each figure the topmost portion is for injection at an angle with the flow (β) of 35^{o} and middle and lowest sections are for lateral injection at angles of 35 and 15 degrees respectively. Thus the degree of lateral injection increases from top to bottom of each figure. At M=0.5, a blowing rate for which the jet is not believed to leave the wall when injected with the flow, Figure 25 shows that the effect of lateral injection is to widen the temperature field while reducing the peak values of the effectiveness. For M=1.0, where the jet is believed to penetrate into the main stream when injected downstream with $\beta=35^{o}$ ($\Phi=90^{o}$), Figure 26 shows that the effect of lateral injection is to both widen the temperature field and increase the maximum effectiveness. Thus, at high blow-

ing rates where the jet leaves the wall when injected downstream ($\beta=35^{o}$, $\Phi=90^{o}$) the introduction of lateral injection will hold the jet closer to the wall and do a more effective job of film cooling.

To illustrate the effect of normal injection, lines of constant film cooling effectiveness for data taken from references 1 and 2 are presented in Figure 27. The upper two diagrams are for injection normal to the flow; the lower two are for injection at an angle of 35^{o} with the flow. The lower two diagrams differ from the upper portions of Figures 25 and 26 because of different values of free stream velocity and hole diameter (cf. Figure 14). The diameter of the injection tubes used in [1] and |2| was 2.35 cm and the free stream velocity for the data in Figure 27 was 61.0 m/s. The data in Figures 25 and 26 was taken with 1.18 cm diameter injection tubes and at a free stream velocity of 30.5 m/s.

VII. RESUME

An experimental investigation has been conducted to determine the adiabatic wall temperature distribution produced by film cooling on a flat plate. An air stream flows along the flat surface forming a turbulent boundary layer, and secondary air is injected into this stream from circular tubes that end flush with the wall. Four different injection systems are used--a single tube inclined at an angle of 35^{o} with the flow, a row of tubes also at an angle of 35^{o}

with the flow and spaced at three diameter intervals, and single tubes at lateral angles of 35 and 15 degrees. The film cooling effectiveness for single hole injection at an angle of 35^{o} with the flow varies not only with position and blowing rate, but also decreases as the dimensionless boundary layer displacement thickness δ^*/D is increased. Little difference in film cooling effectiveness between single hole and multiple hole injection is observed for M=0.5. The effectiveness for multiple holes, comparing it with the predictions from the single hole experiments by superposition, is significantly higher at higher blowing rates. The effect of lateral injection through a single hole is to widen the temperature field and to decrease the peak effectiveness for the low blowing rate (M=0.5) in which the jet remains near the wall in any arrangement. For higher blowing rates in which the jet penetrates into the mainstream, lateral injection holds the jet closer to the wall, thus increasing both the width of the temperature field and the peak film cooling effectiveness.

ACKNOWLEDGMENTS

The authors wish to express their appreciation to T.C. Nelson and R.H. Kolar for their aid during the course of the investigation and to Frank Stepka of the Lewis Laboratory NASA for his valuable suggestions.

REFERENCES

|1| Goldstein, R.J., E.R.G. Eckert, and J.W. Ramsey, "Film Cooling with Injection Through Holes: Adiabatic Wall Temperatures Downstream of a Circular Hole," Journal of Engineering for Power, Trans. ASME, Series A, Vol. 90, No. 4, October 1968, pp. 384-395.

|2| Goldstein, R.J., E.R.G. Eckert, and J.W. Ramsey, "Film Cooling with Injection Through a Circular Hole," NASA CR-56404, May 1968. (also University of Minnesota Heat Transfer Laboratory TR No. 82.)

|3| Wieghardt, K., "Hot-Air Discharge for De-icing," AAF Translation, Report No. F-TS-919-Re, Wright Field (1946).

|4| Chin, J.H., S.C. Skirvin, L.E. Hayes, and F. Burggraf, "Film Cooling with Multiple Slots and Louvers," Journal of Heat Transfer, Trans. ASME, Series C., Vol. 83, August 1961, pp. 281-292.

|5| Metzger, D.E., and D.D. Fletcher, "Surface Heat Transfer Immediately Downstream of Flush, Non-Tangential Injection Holes and Slots," AIAA Paper No. 69-523, 1969.

|6| Goldstein, R.J. and A. Haji-Sheikh, "Prediction of Film Cooling Effectiveness," JSME 1967 Semi-International Symposium, 4th-8th September, 1967, pp. 213-218.

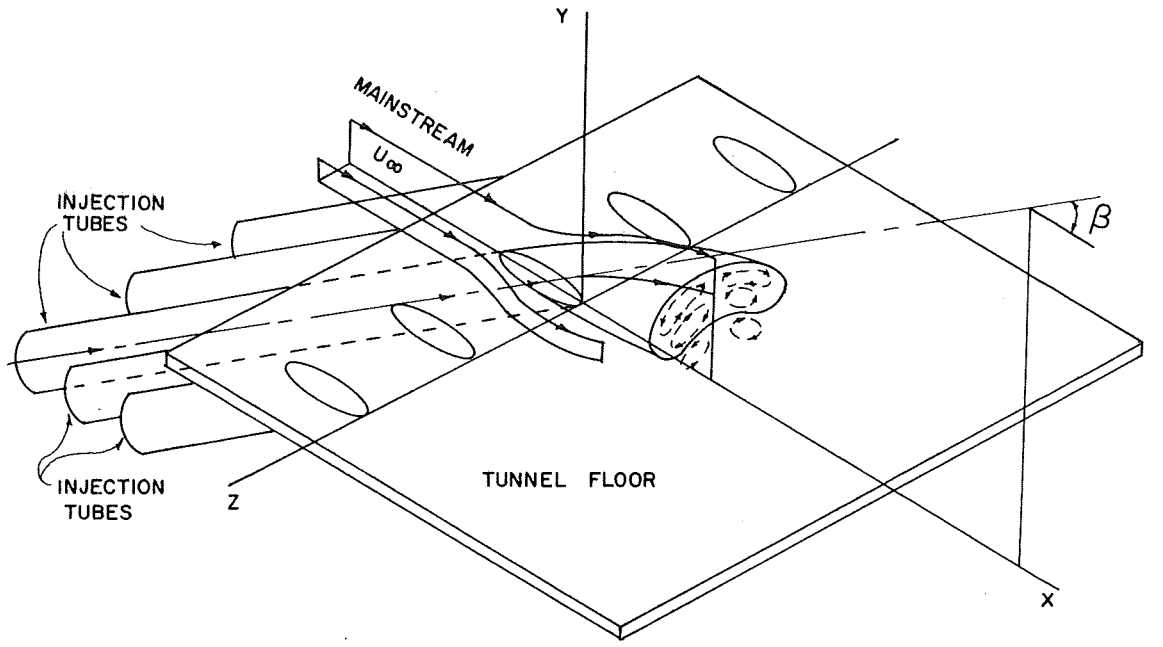

Fig. 1(a) Injection segment and coordinate system for a row of inclined jets. Detail and flow field are shown for only a single jet interacting with a mainstream.

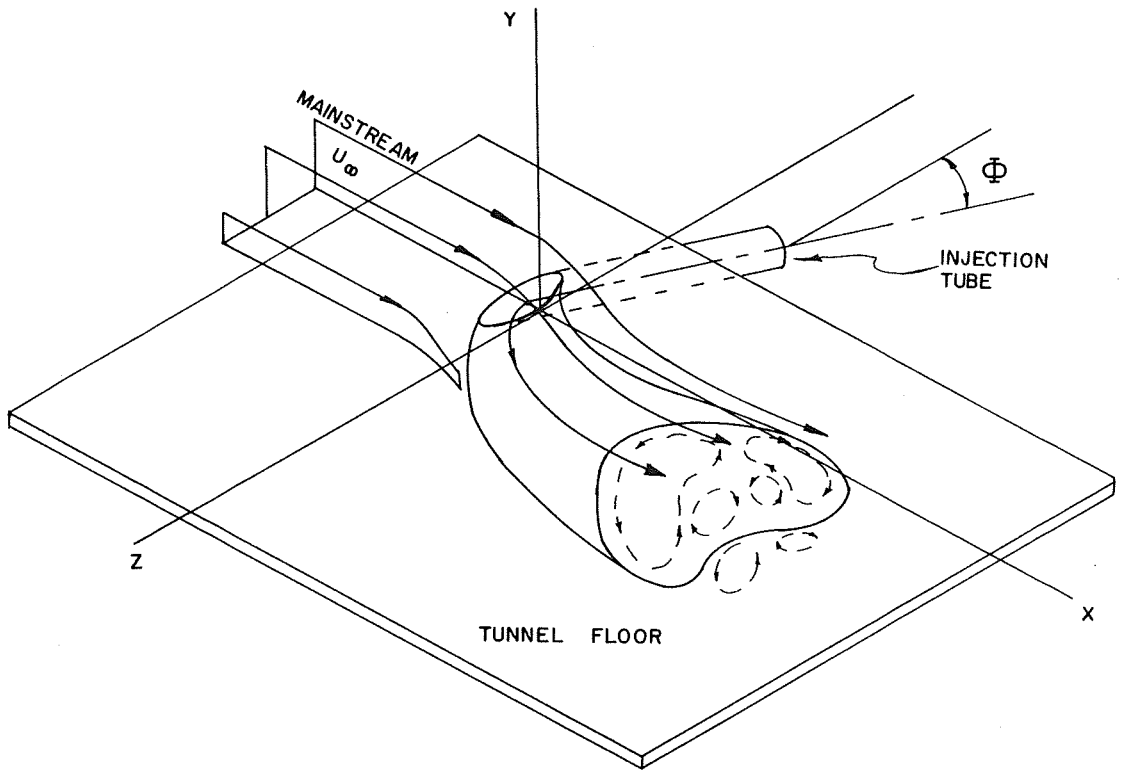

Fig. 1(b) Flow field and coordinate system associated with a laterally inclined jet interacting with a mainstream.

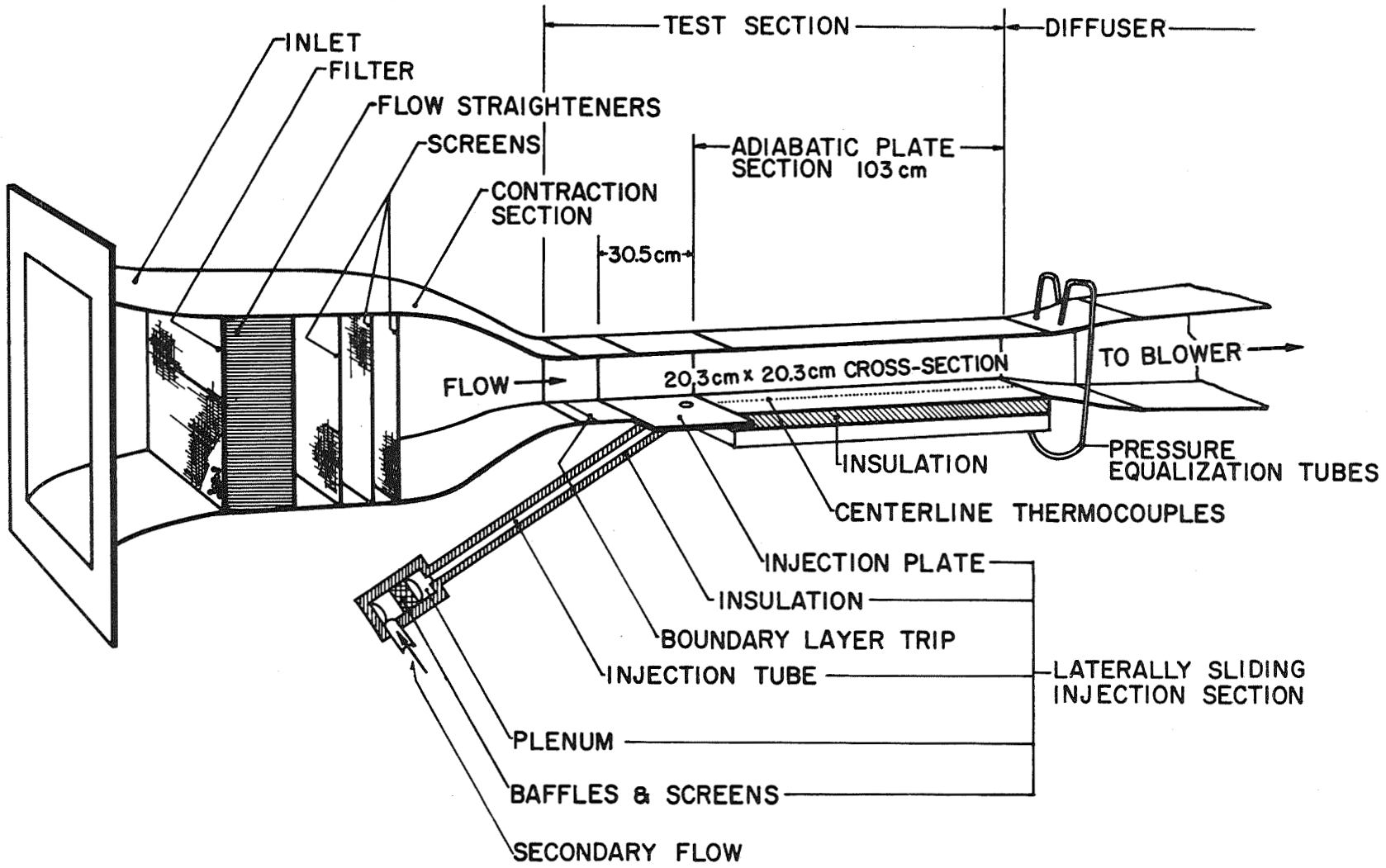

Fig. 2 Wind tunnel.

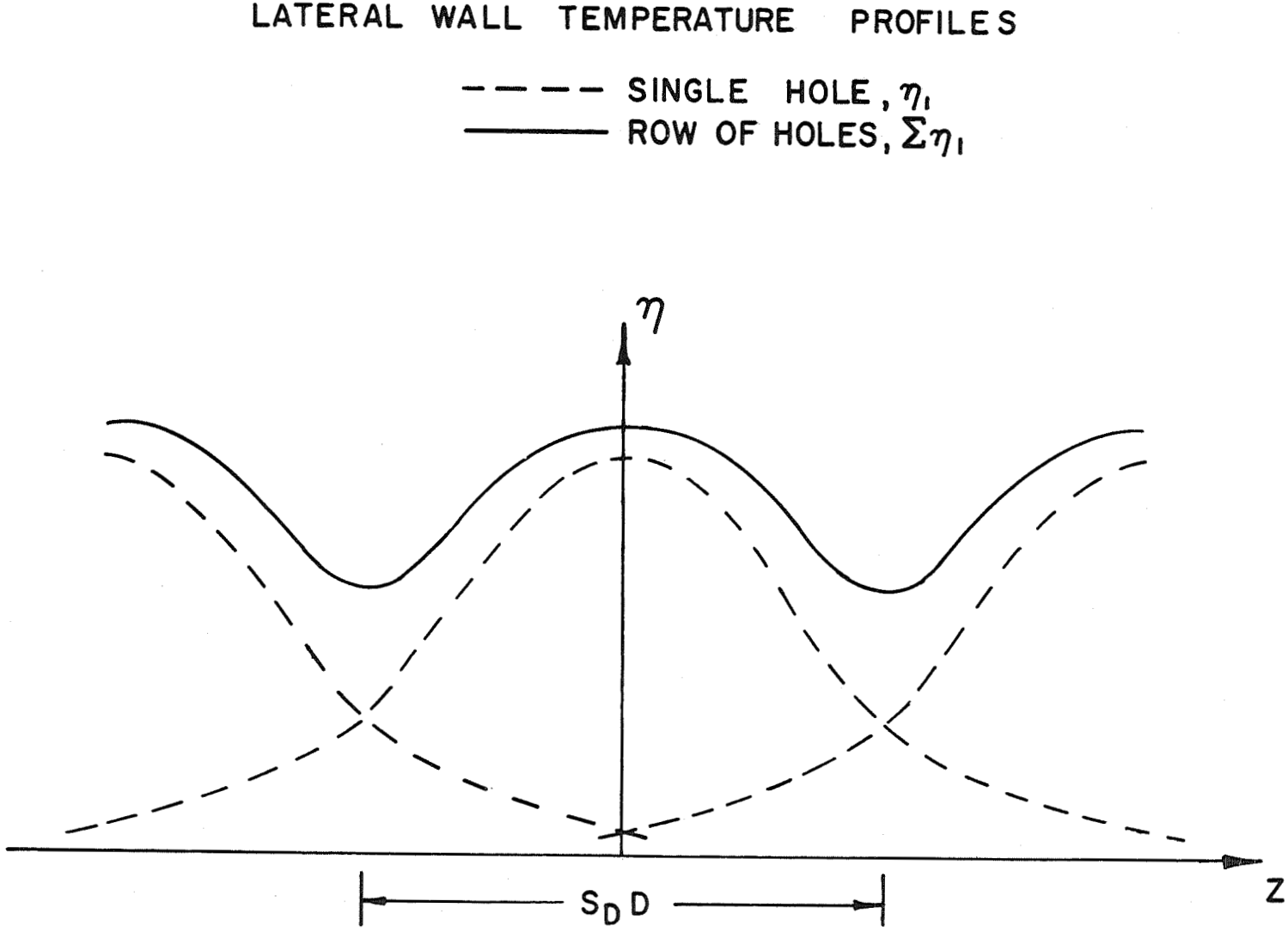

Fig. 3 Superposition of single hole results to predict local effectiveness for injection through a row of holes.

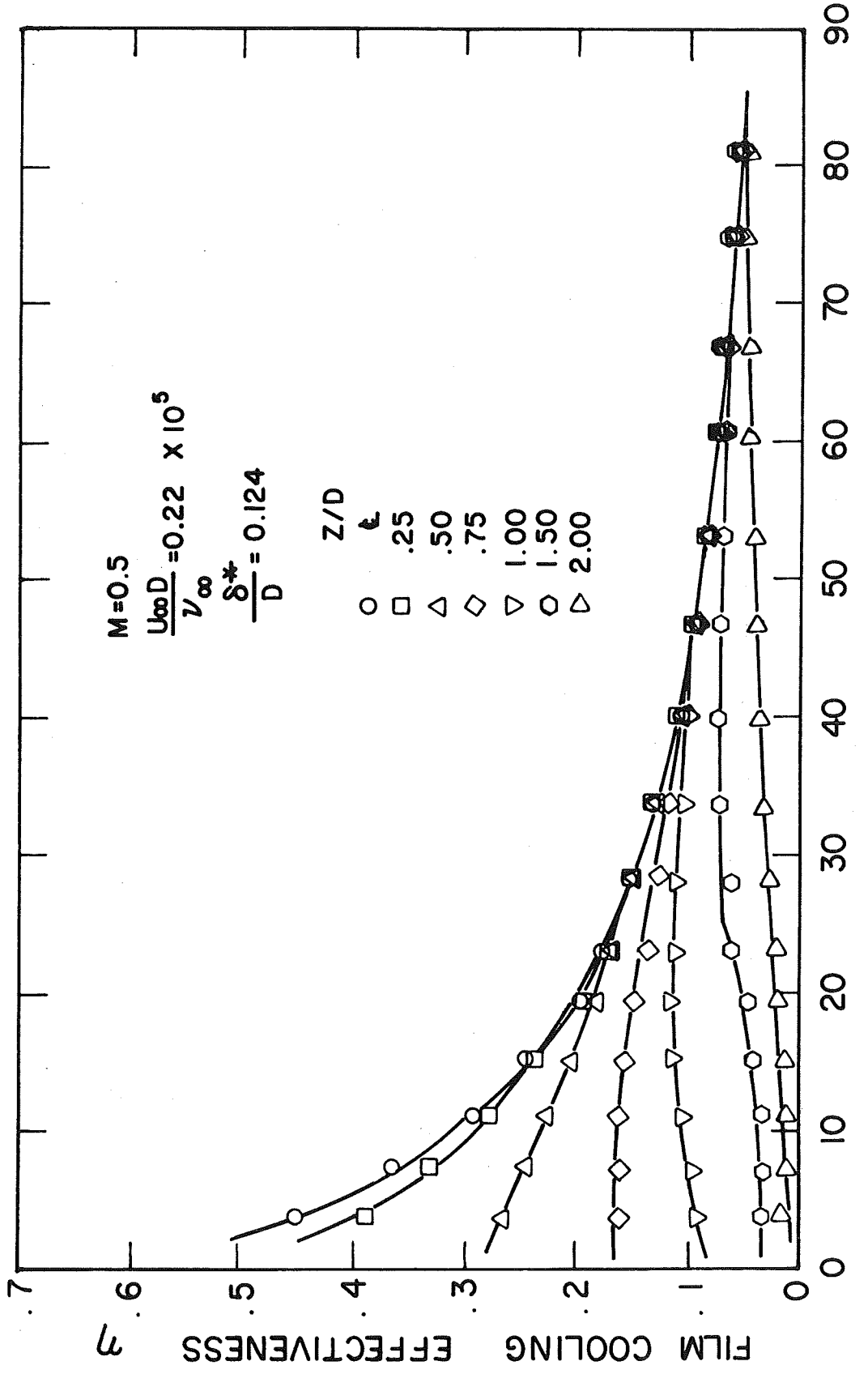

Fig. 4 Axial film cooling effectiveness distributions for injection through a single hole at an angle of 35° with the main flow, U_∞=30.5 m/s, M=0.5.

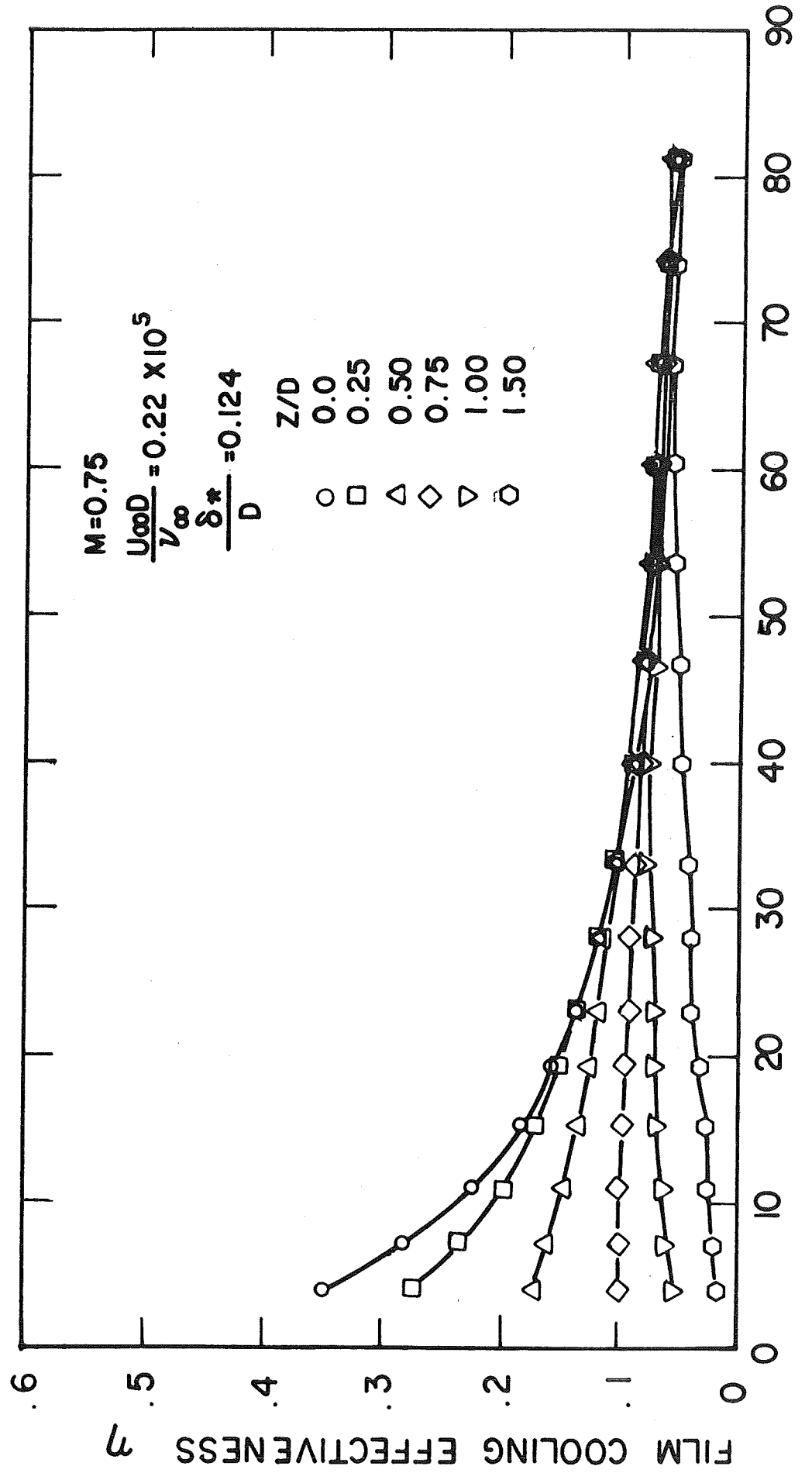

Fig. 5 Axial film cooling effectiveness distributions for injection through a single hole at an angle of 35° with the main flow, U_∞=30.5 m/s, M=0.75.

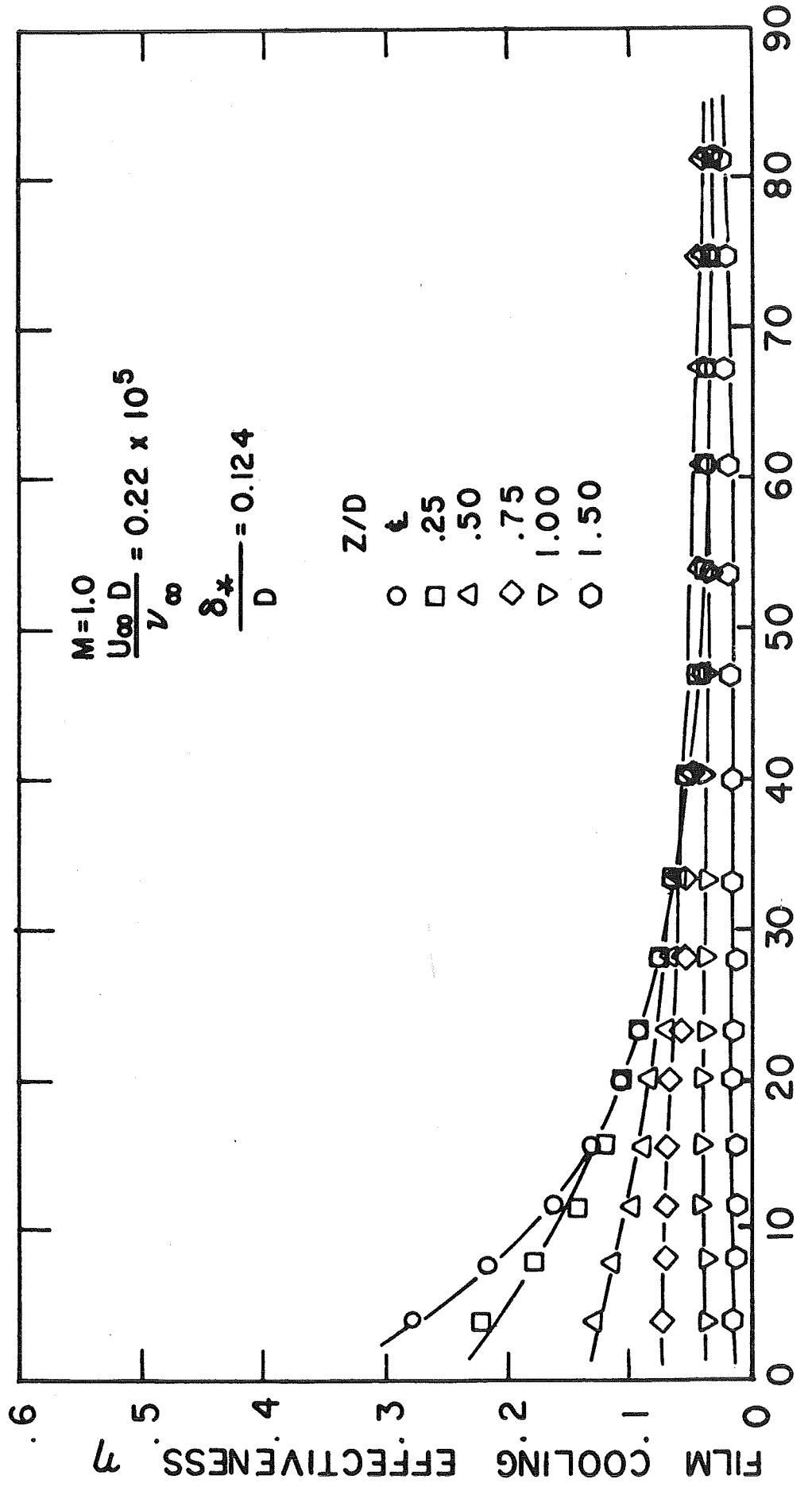

Fig. 6 Axial film cooling effectiveness distributions for injection through a single hole at an angle of 35° with the main flow, U_∞=30.5 m/s, M=1.0.

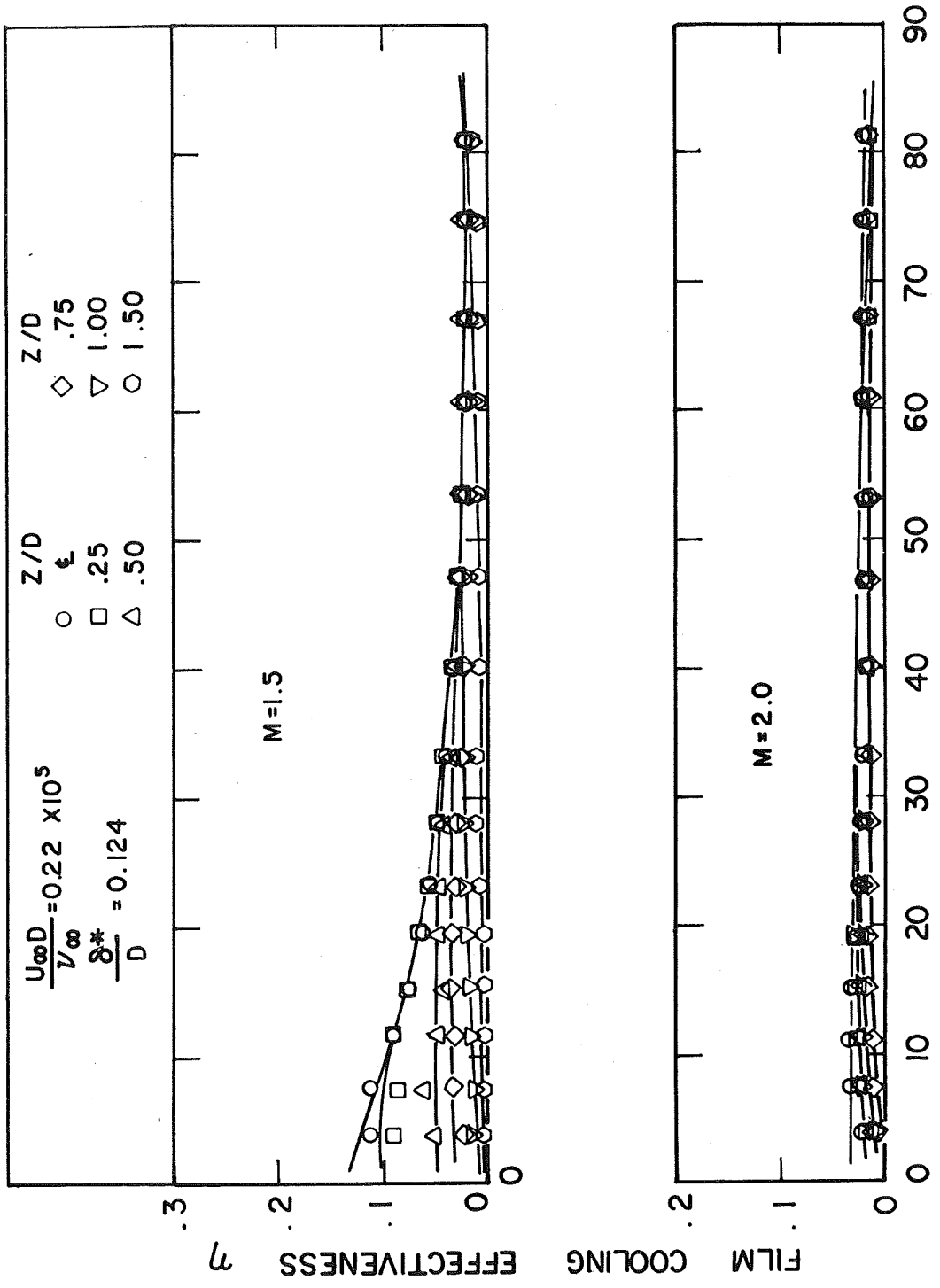

Fig. 7 Axial film cooling effectiveness distributions for injection through a single hole at an angle of 35^0 with the main flow, U_∞=30.5 m/s, M=1.5 and 2.0.

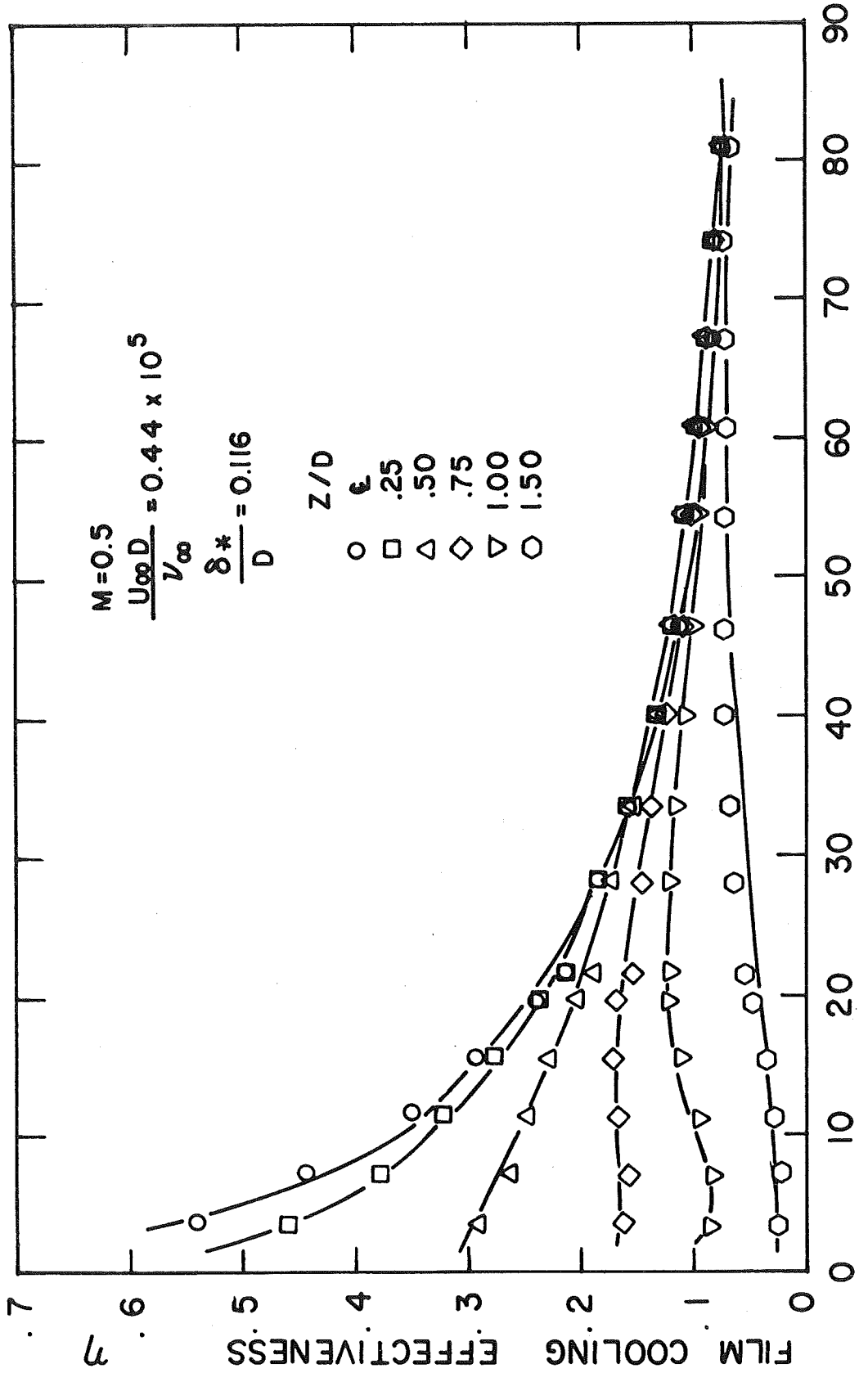

Fig. 8 Axial film cooling effectiveness distributions for injection through a single hole at an angle of 35° with the main flow, U_∞=61.0 m/s, M=0.5.

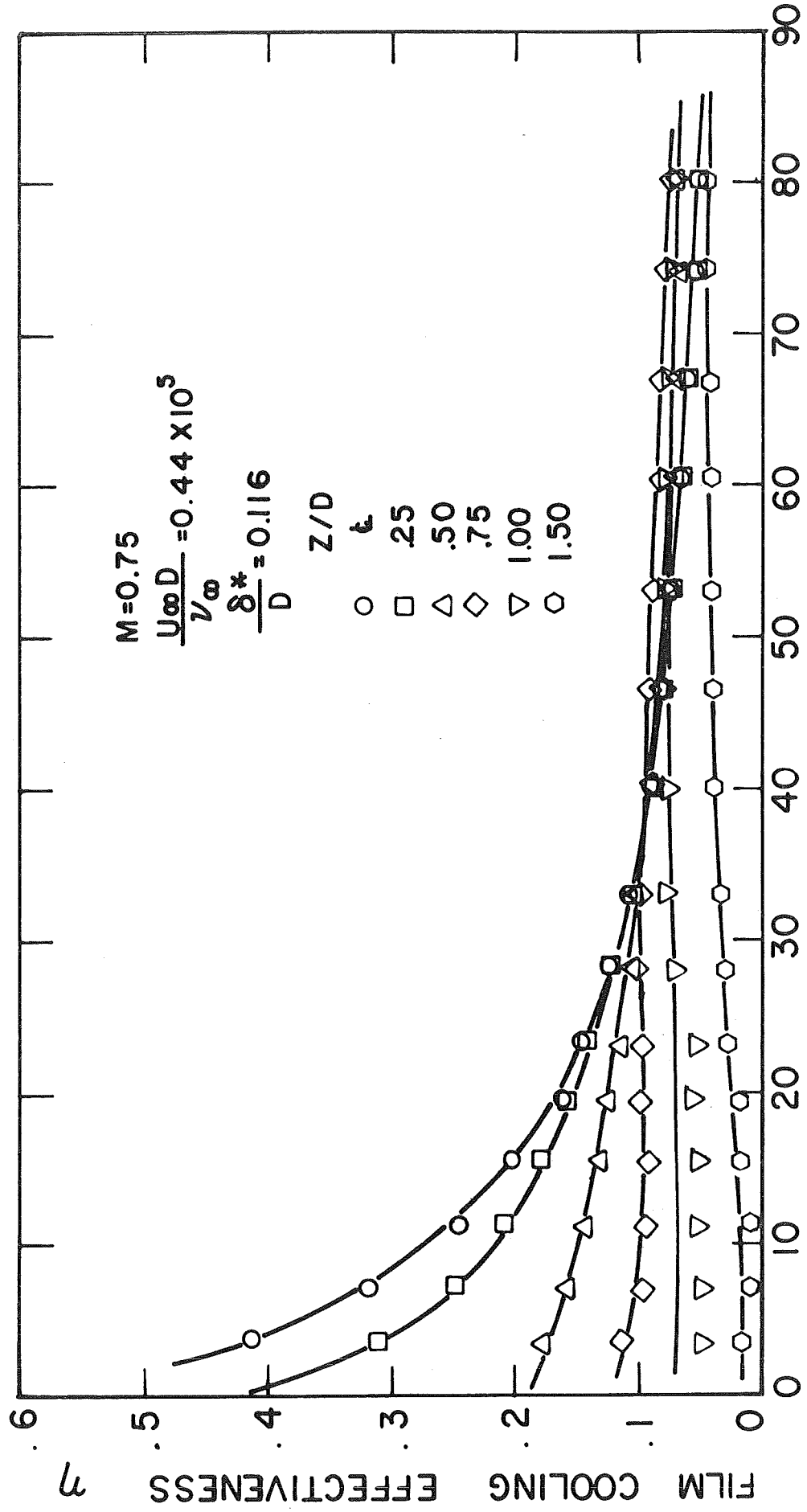

Fig. 9 Axial film cooling effectiveness distributions for injection through a single hole at an angle of 35^o with the main flow, U_∞=61.0 m/s, M=0.75.

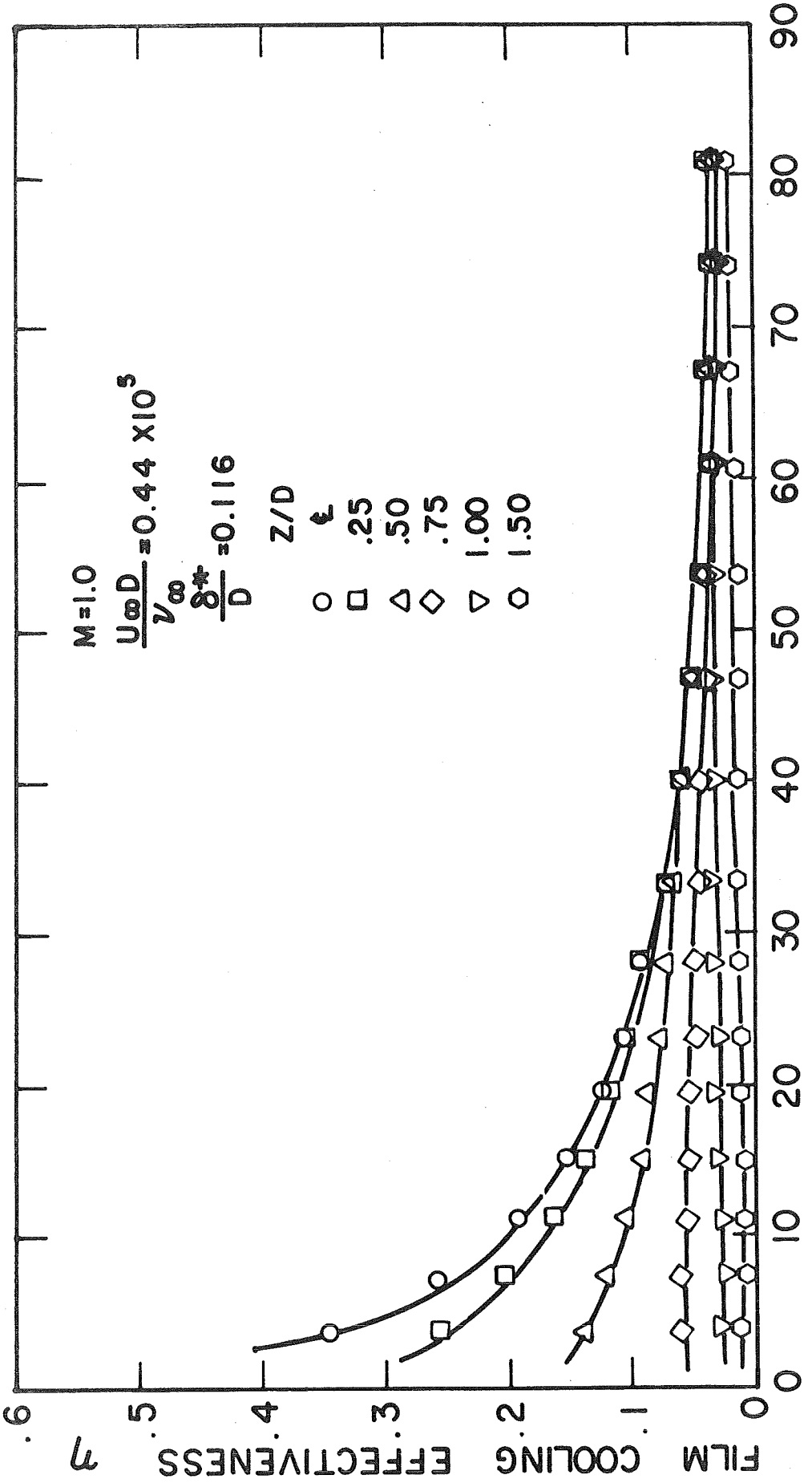

Fig. 10 Axial film cooling effectiveness distributions for injection through a single hole at an angle of 35° with the main flow, U_∞=61.0 m/s, M=1.0.

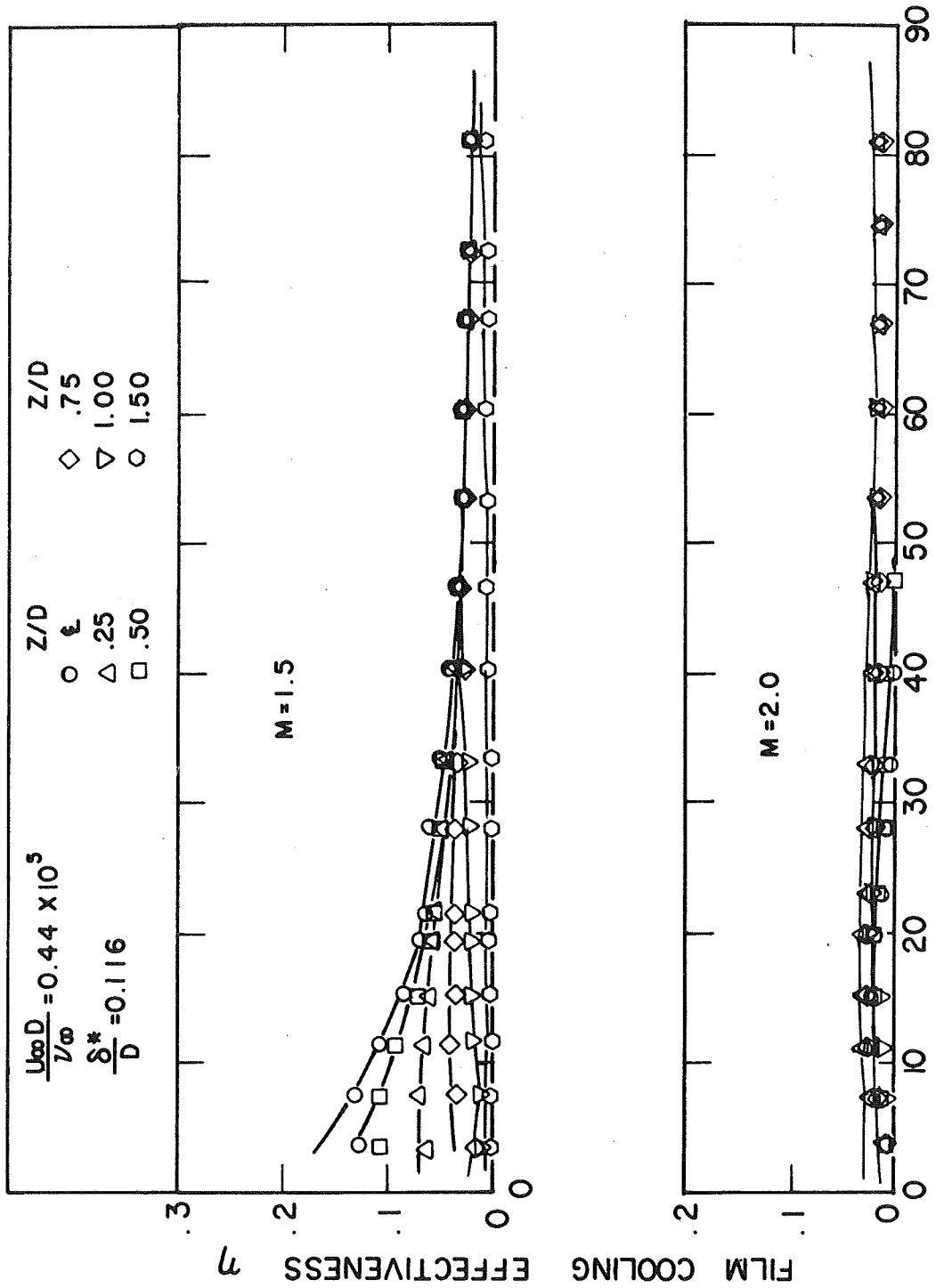

Fig. 11 Axial film cooling effectiveness distributions for injection through a single hole at an angle of 35° with the main flow, U_∞=61.0 m/s, M=1.5 and 2.0.

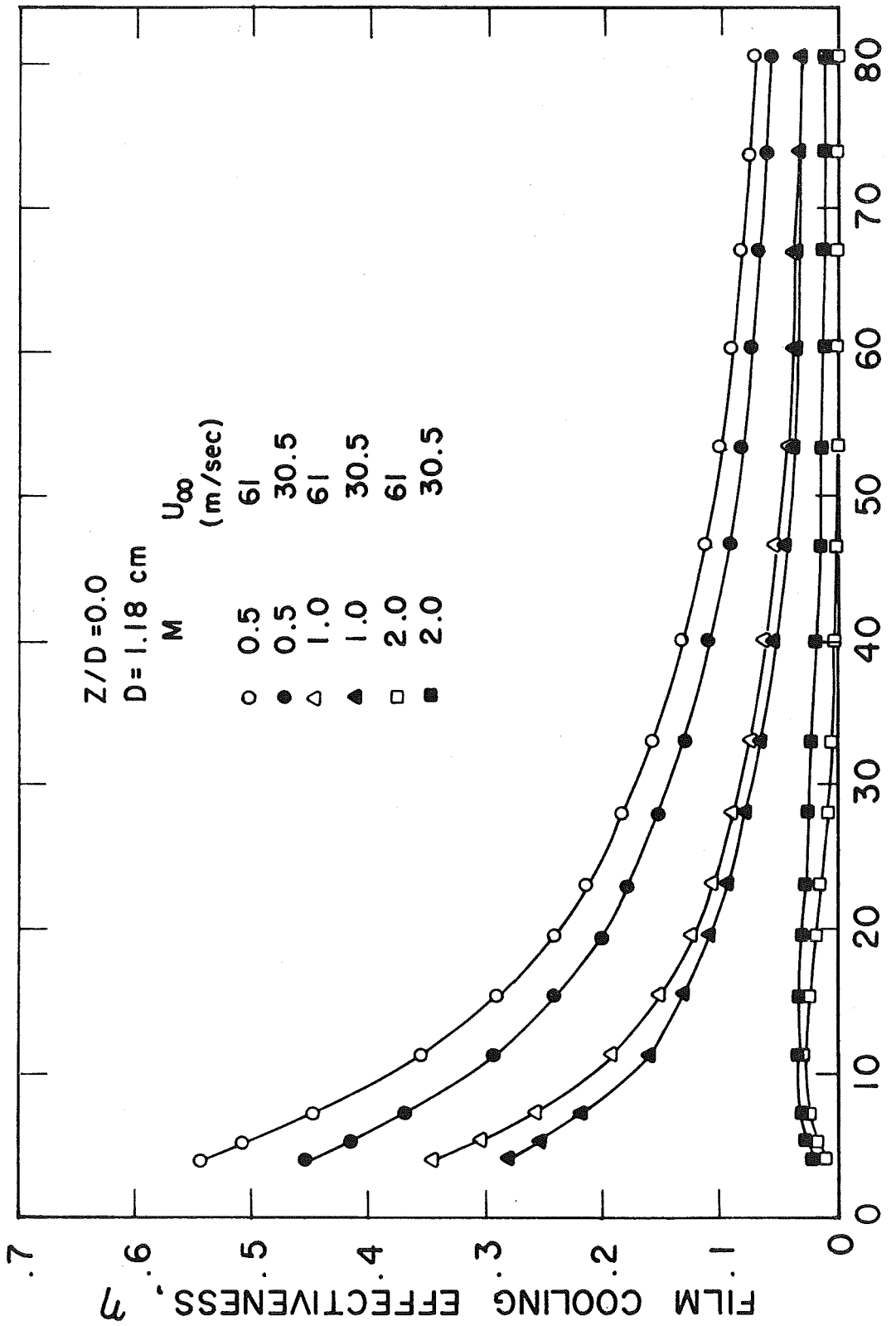

Fig. 12 The effect of freestream velocity on the centerline film cooling effectiveness for single hole injection at an angle of 35^{0} with the flow.

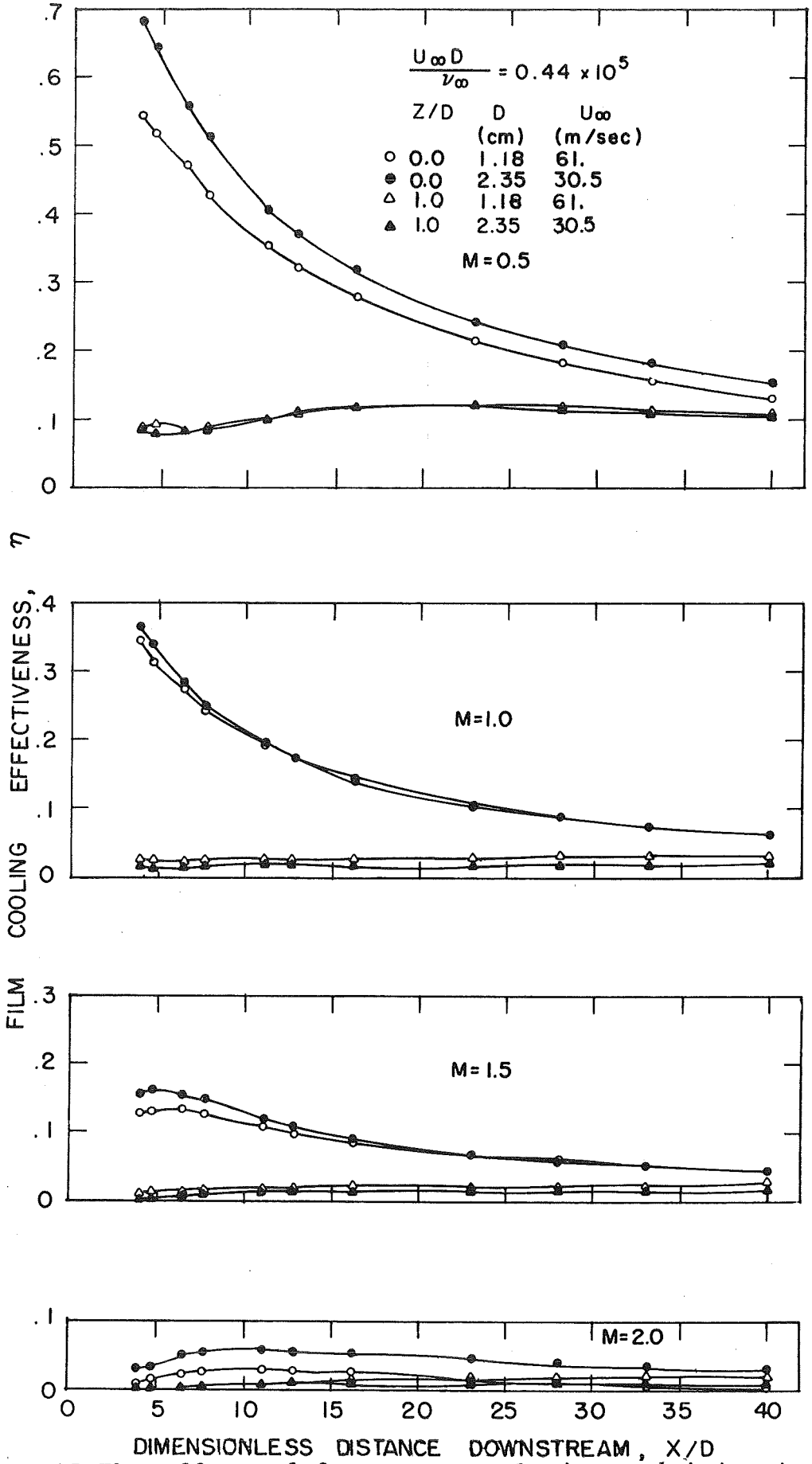

Fig. 13 The effect of freestream velocity and injection tube diameter at constant $U_\infty D/\nu$ on axial film cooling effectiveness distributions for single hole injection at an angle of 35° with the flow.

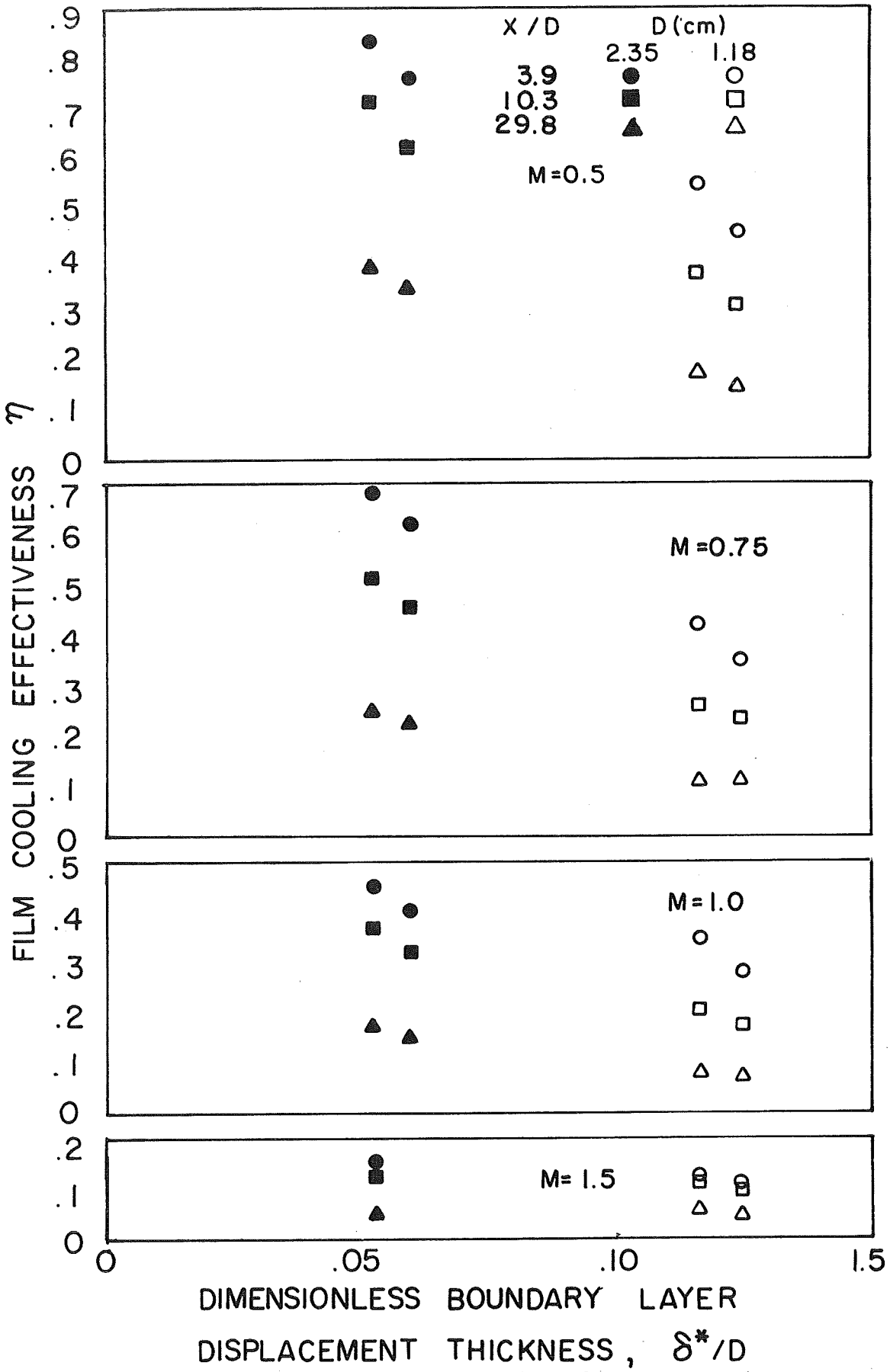

Fig. 14 The effect of dimensionless boundary layer displacement thickness on centerline film cooling effectiveness for injection through a single hole at an angle of 35° with the flow.

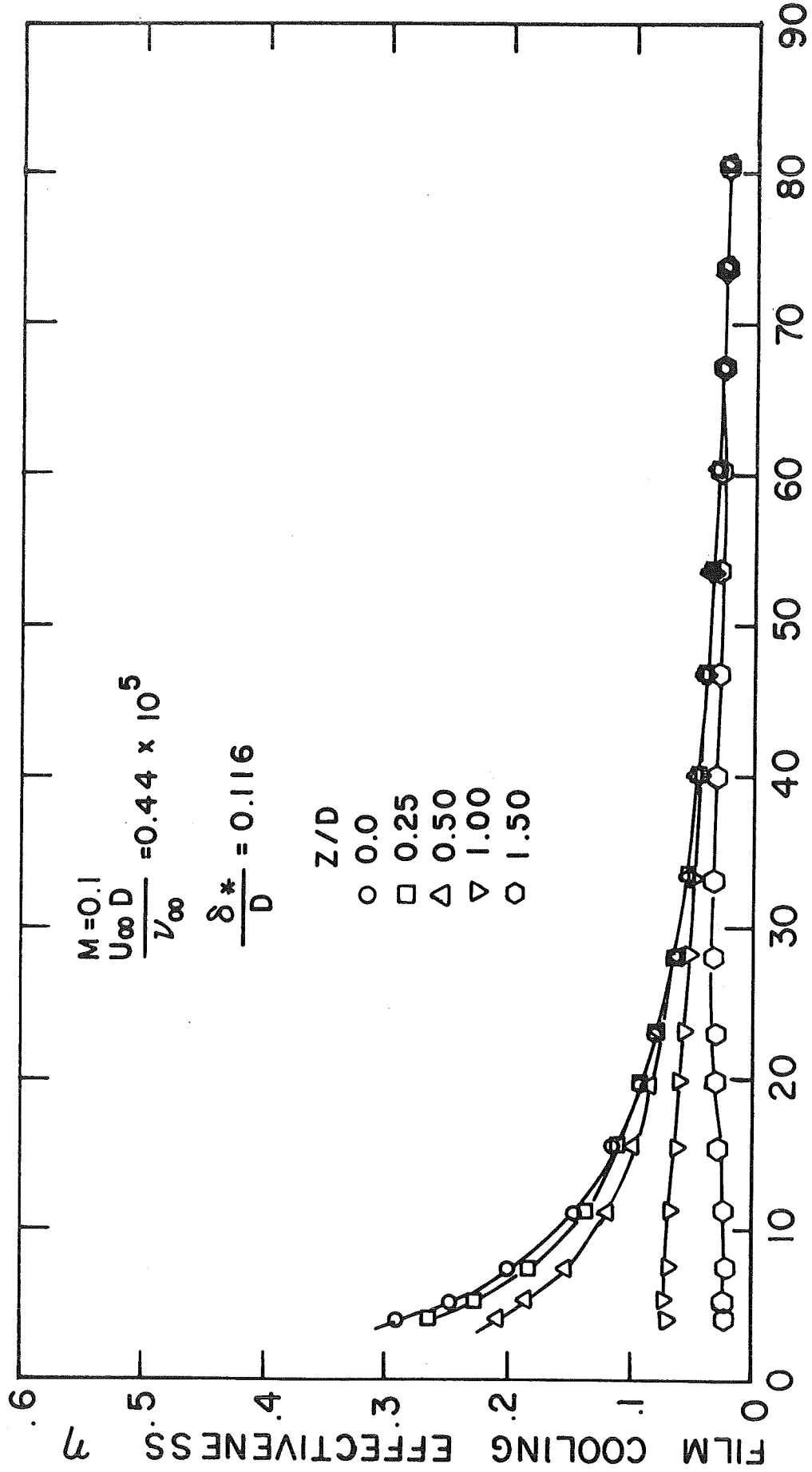

Fig. 15 Axial film cooling effectiveness distribution for injection through a row of holes at an angle of 35^0 with the main flow, U_∞=61.0 m/s, M=0.1.

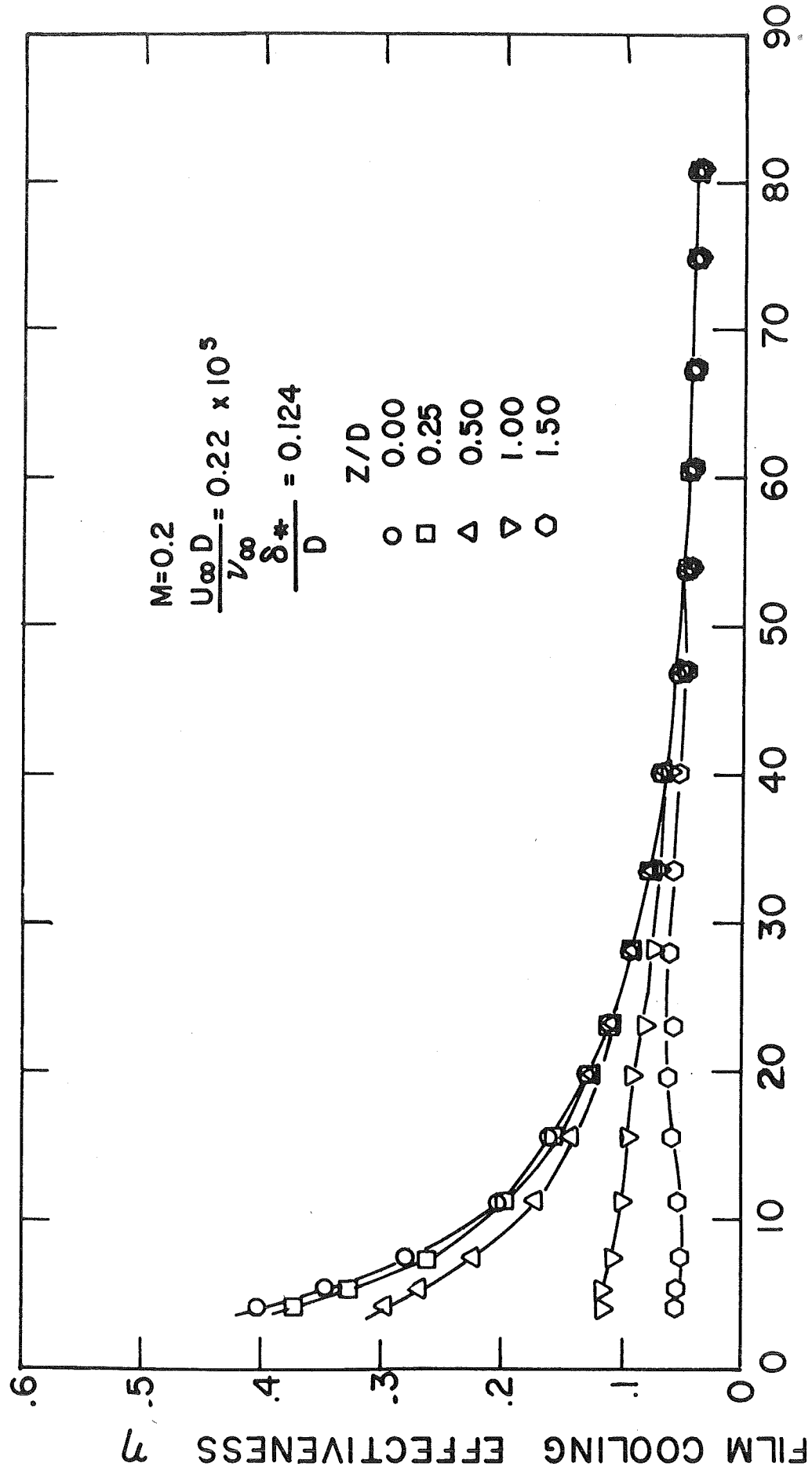

Fig. 16 Axial film cooling effectiveness distributions for injection through a row of holes at an angle of 35^0 with the main flow, U_∞=30.5 m/s, M=0.2.

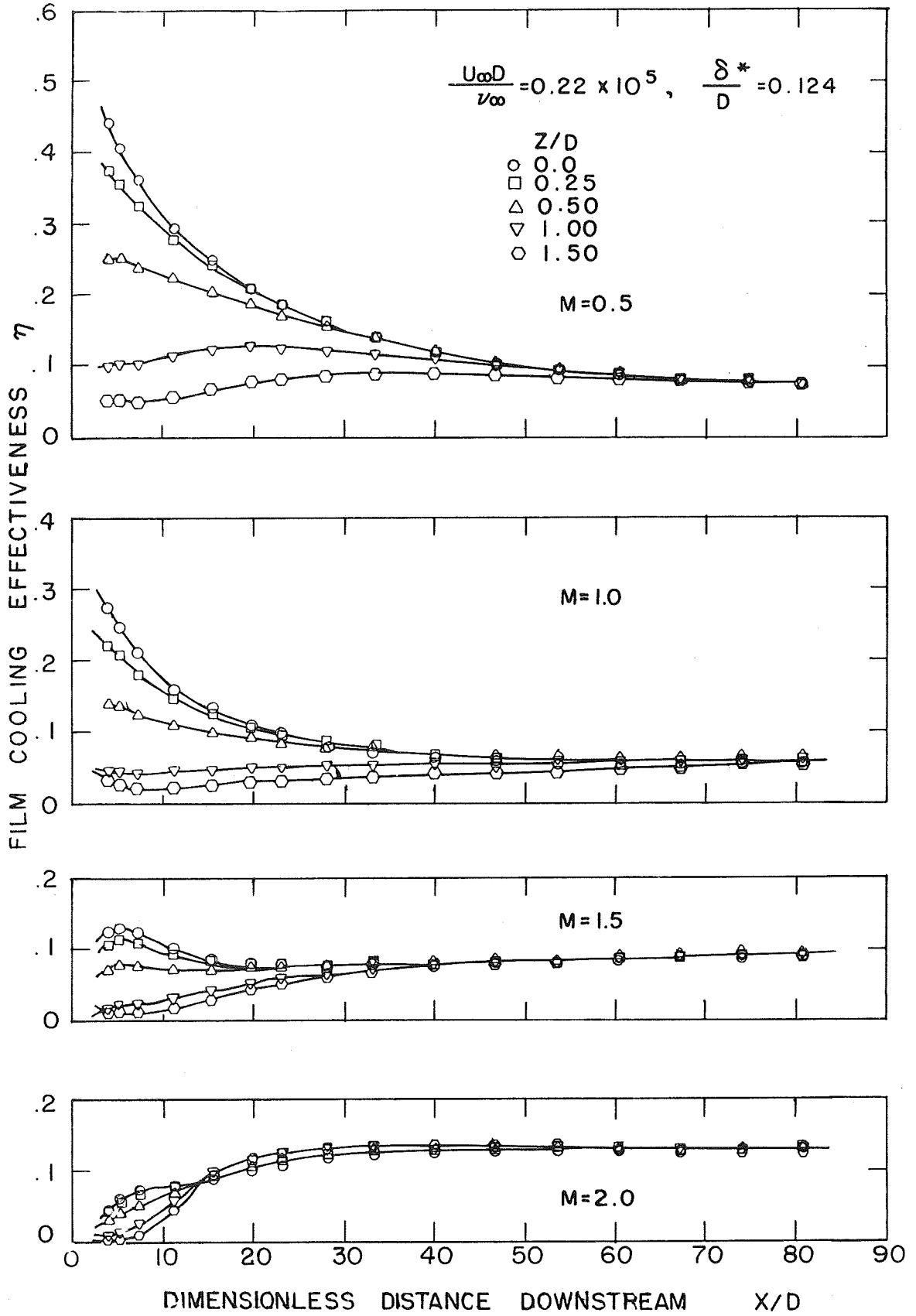

Fig. 17 Axial film cooling effectiveness distributions for injection through a row of holes at an angle of 35° with the main flow, U_∞=30.5 m/s, M=0.5, 1.0, 1.5, 2.0.

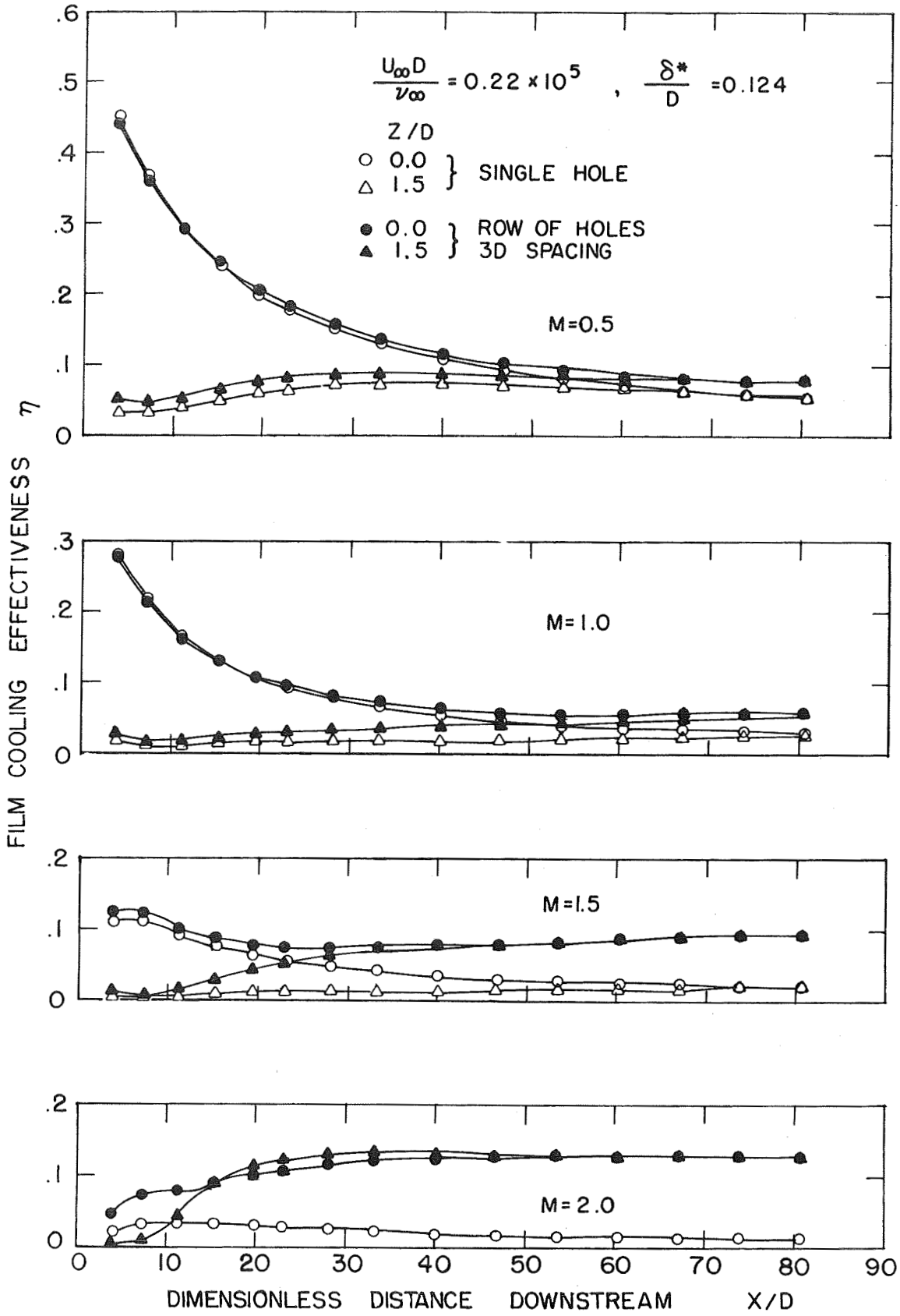

Fig. 18 Comparison of single and multiple hole injection for injection through holes at an angle of 35° with the flow.

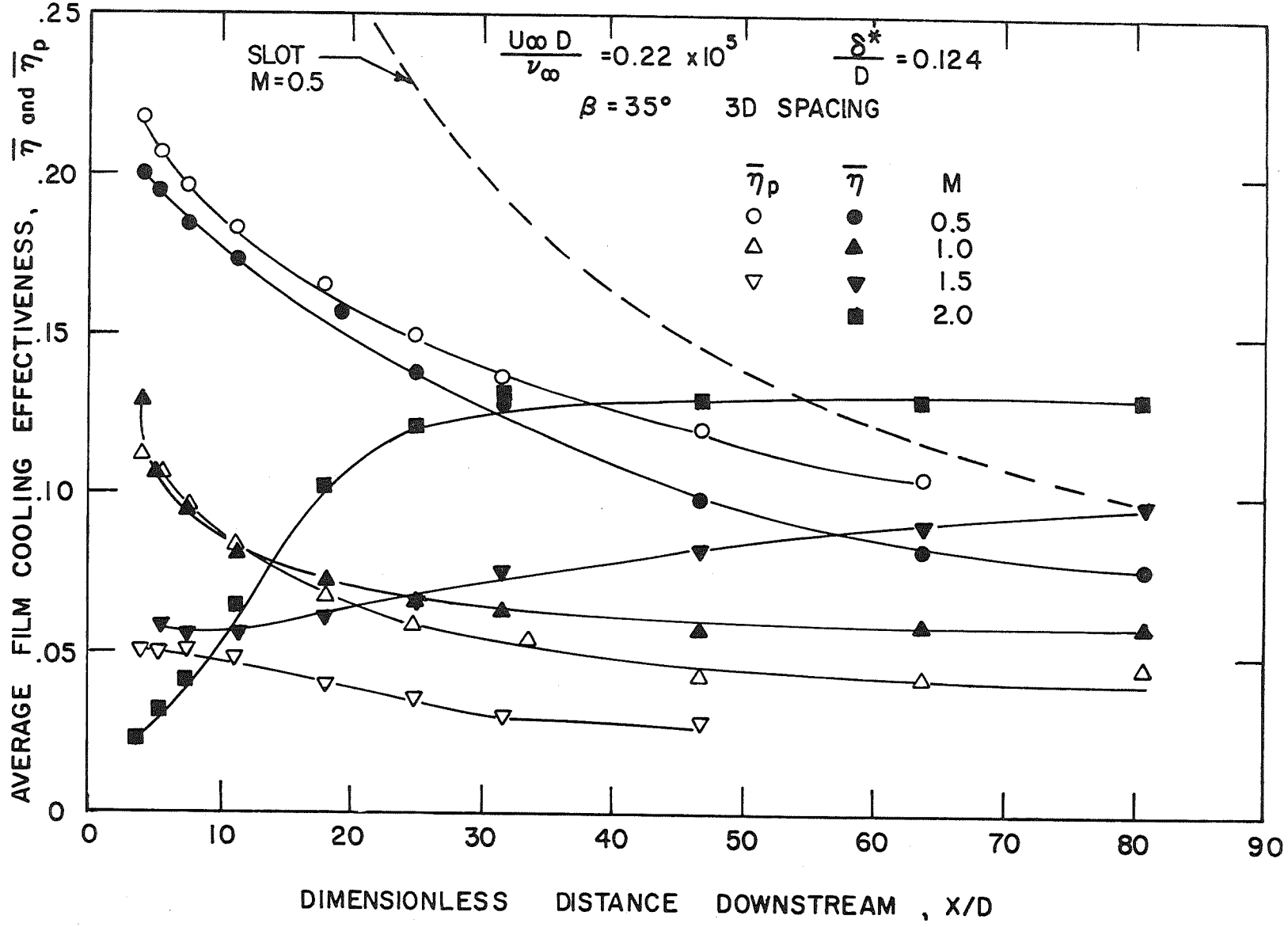

Fig. 19 Comparison of the laterally averaged film cooling effectiveness for a row of holes with that predicted by superimposed single hole measurements.

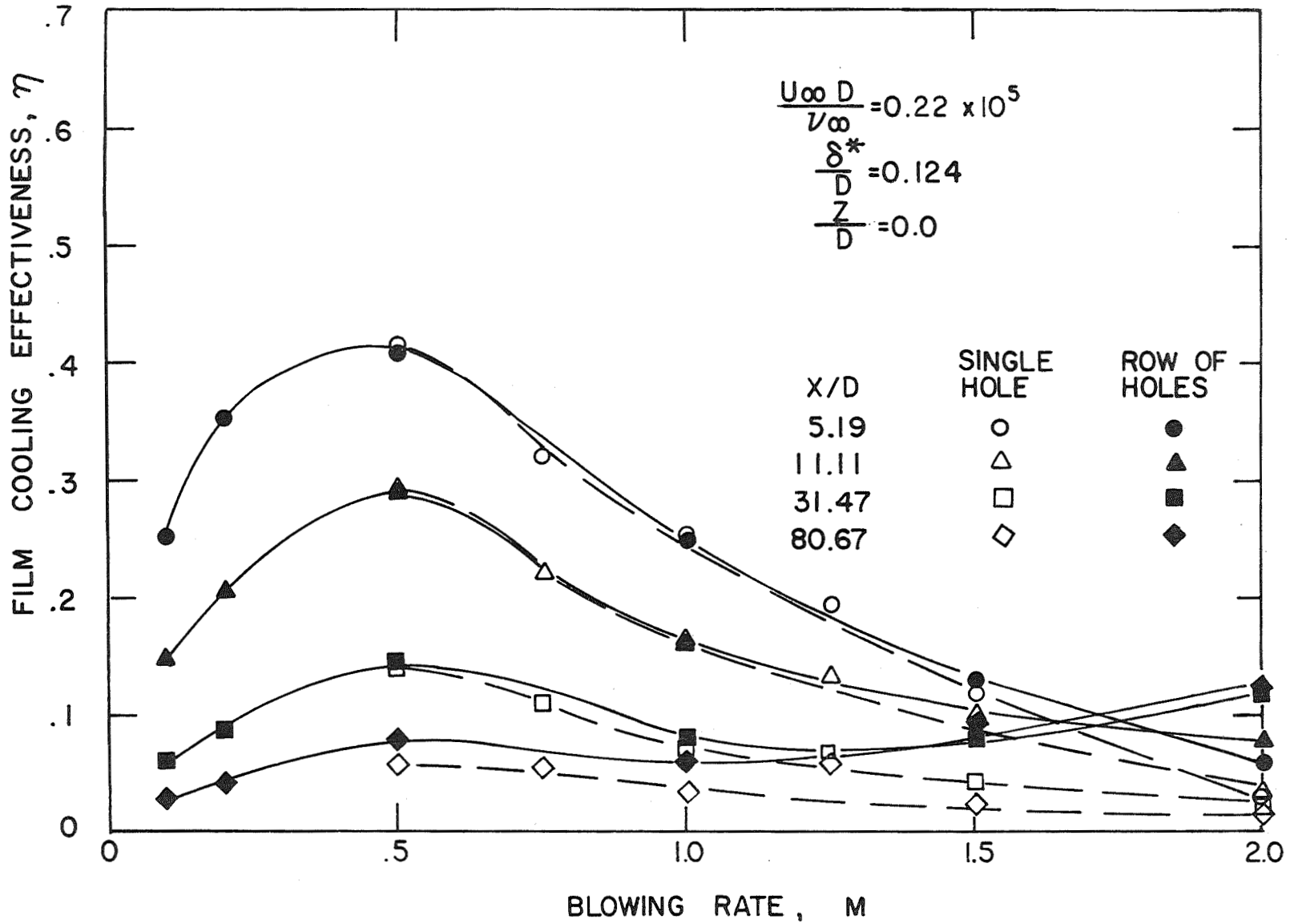

Fig. 20 Effect of blowing rate on centerline film cooling effectiveness for single hole and multiple hole injection at an angle of 35^{0} with the flow.

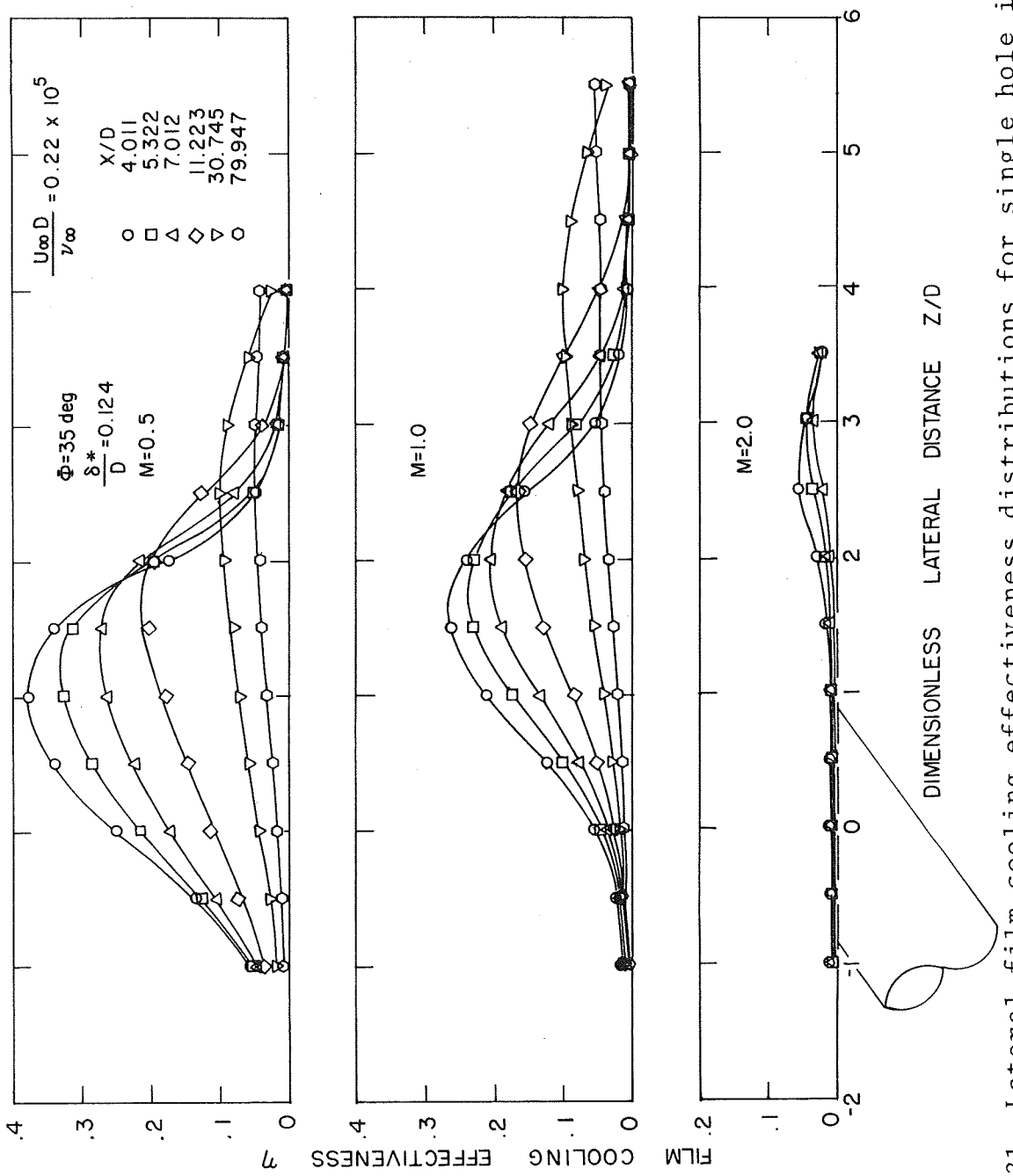

Fig. 21 Lateral film cooling effectiveness distributions for single hole injection at a lateral angle of 35° to the flow.

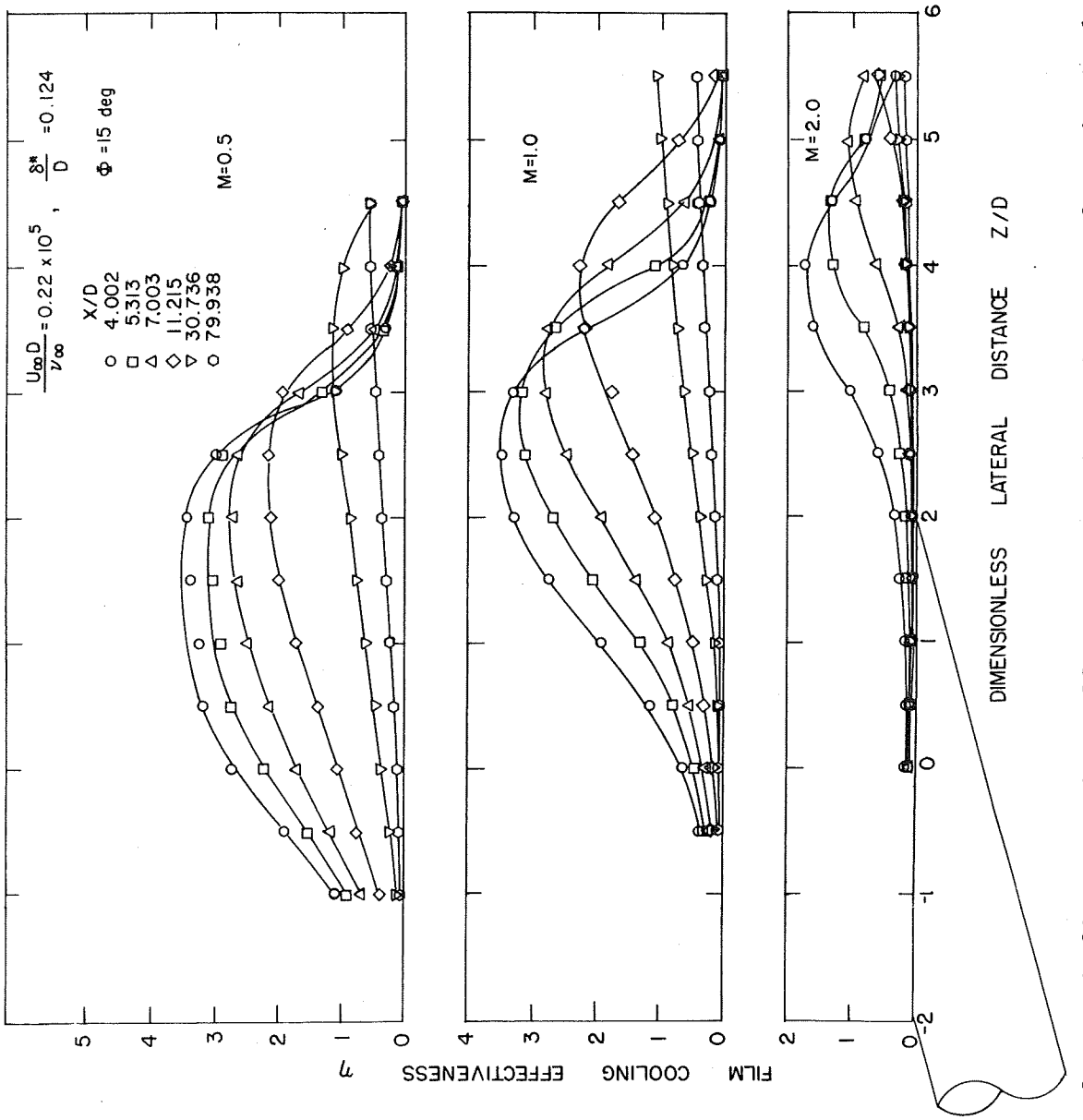

Fig. 22 Lateral film cooling effectiveness distributions for single hole injection at a lateral angle of 15 degrees.

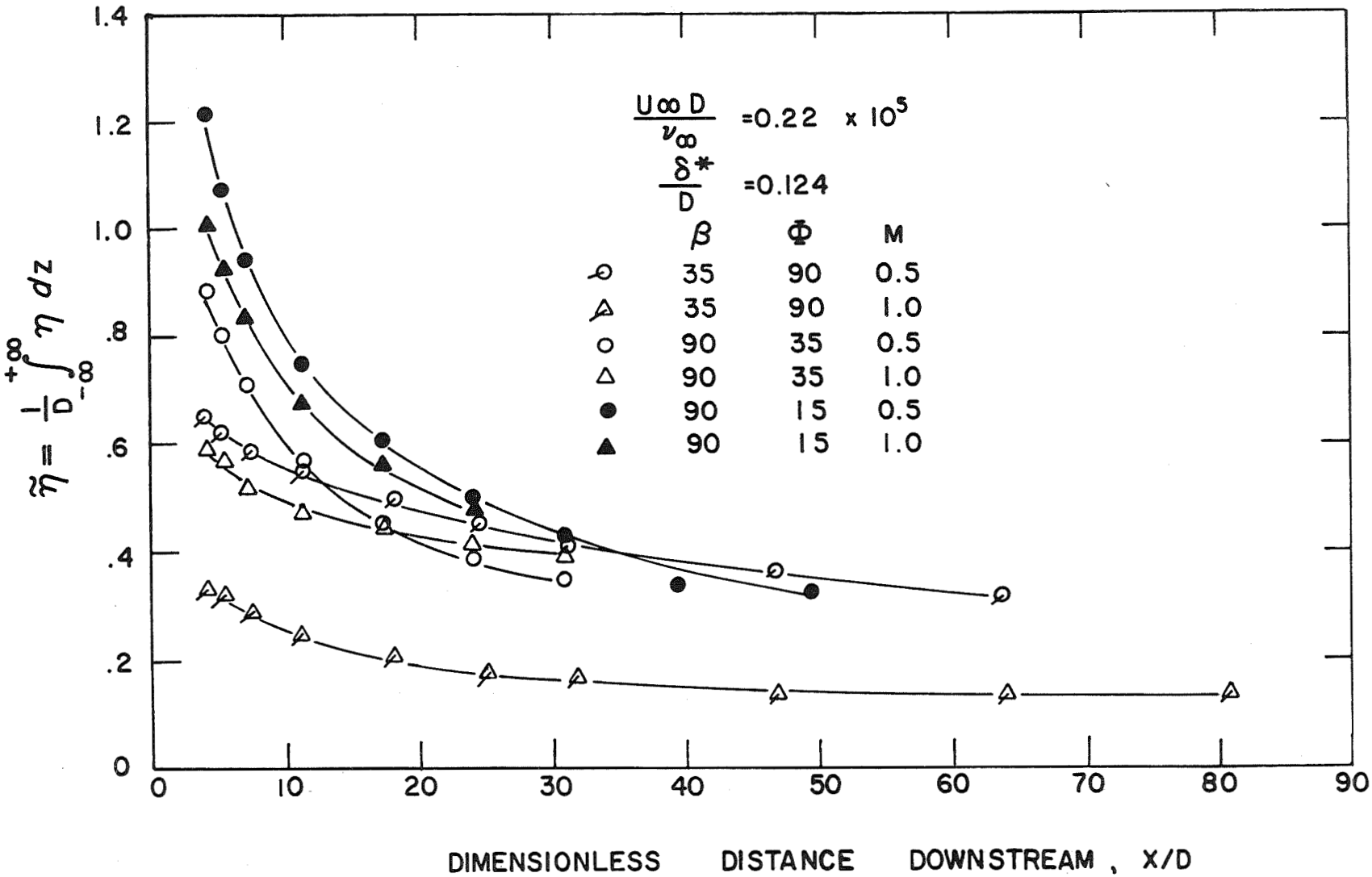

Fig. 23 Comparison of the lateral integral of the film cooling effectiveness for single hole injection at an angle of 35^o with the flow and at lateral angles of 35^o and 15^o.

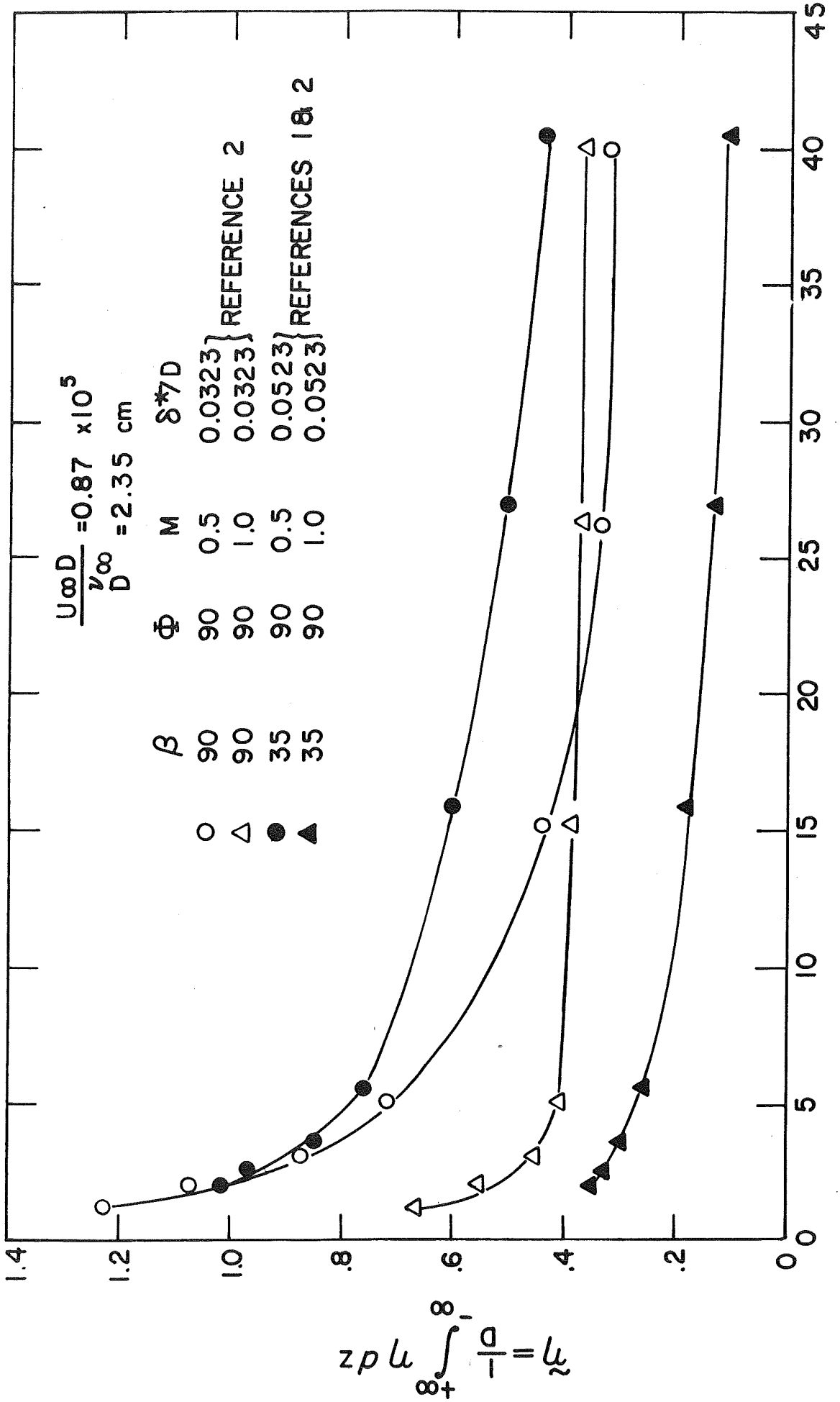

Fig. 24 Lateral integral of the film cooling effectiveness for normal injection and injection at 35° with the flow.

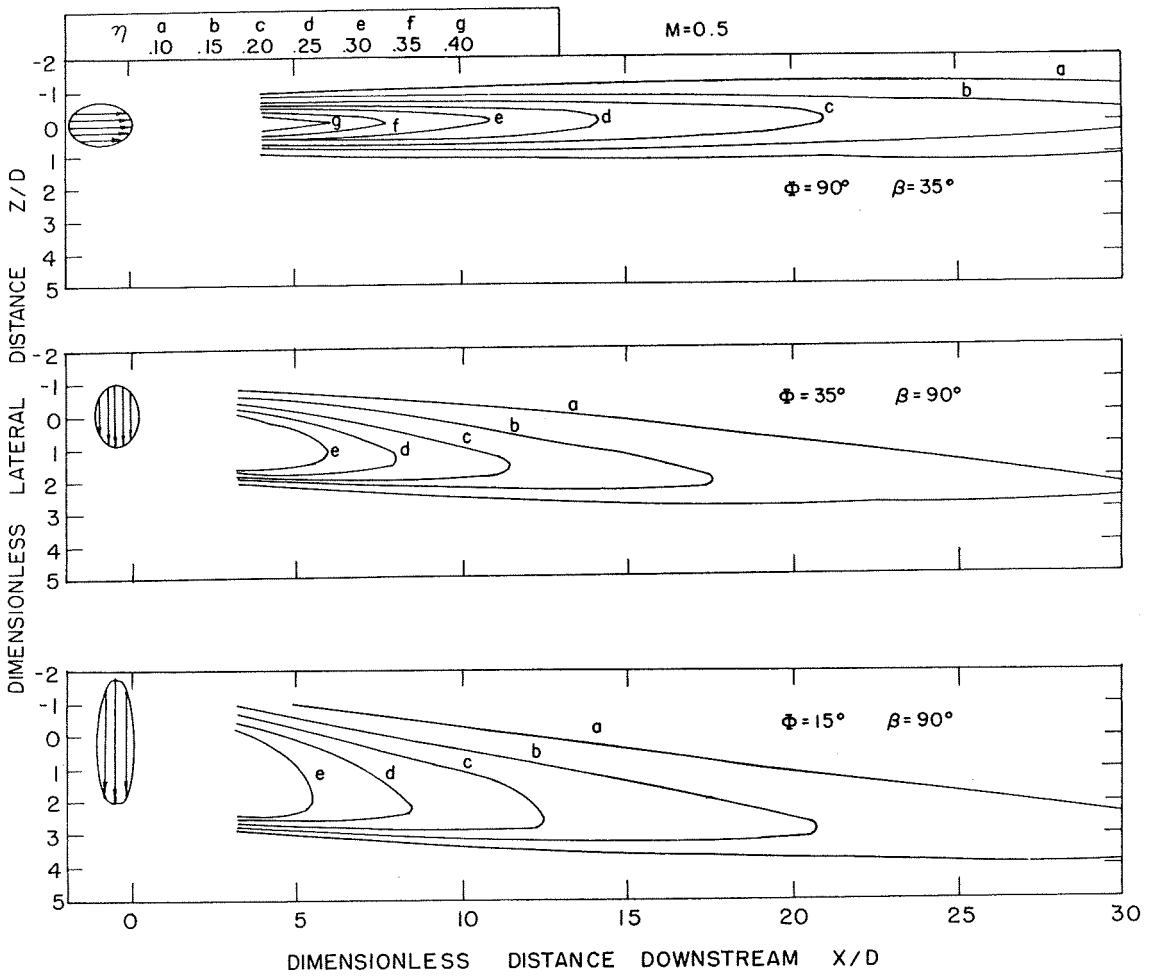

Fig. 25 Lines of constant film cooling effectiveness for single hole injection at M=0.5.

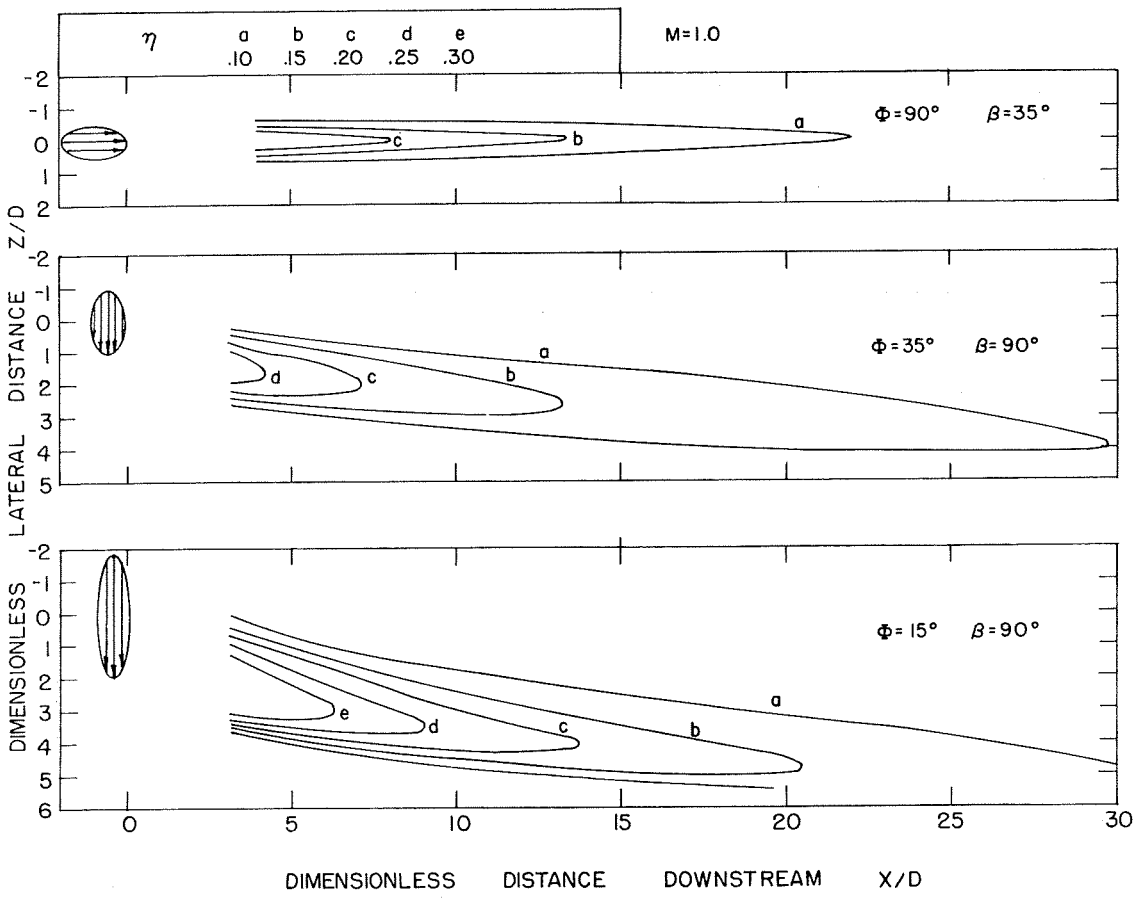

Fig. 26 Lines of constant film cooling effectiveness for single hole injection at M=1.0.

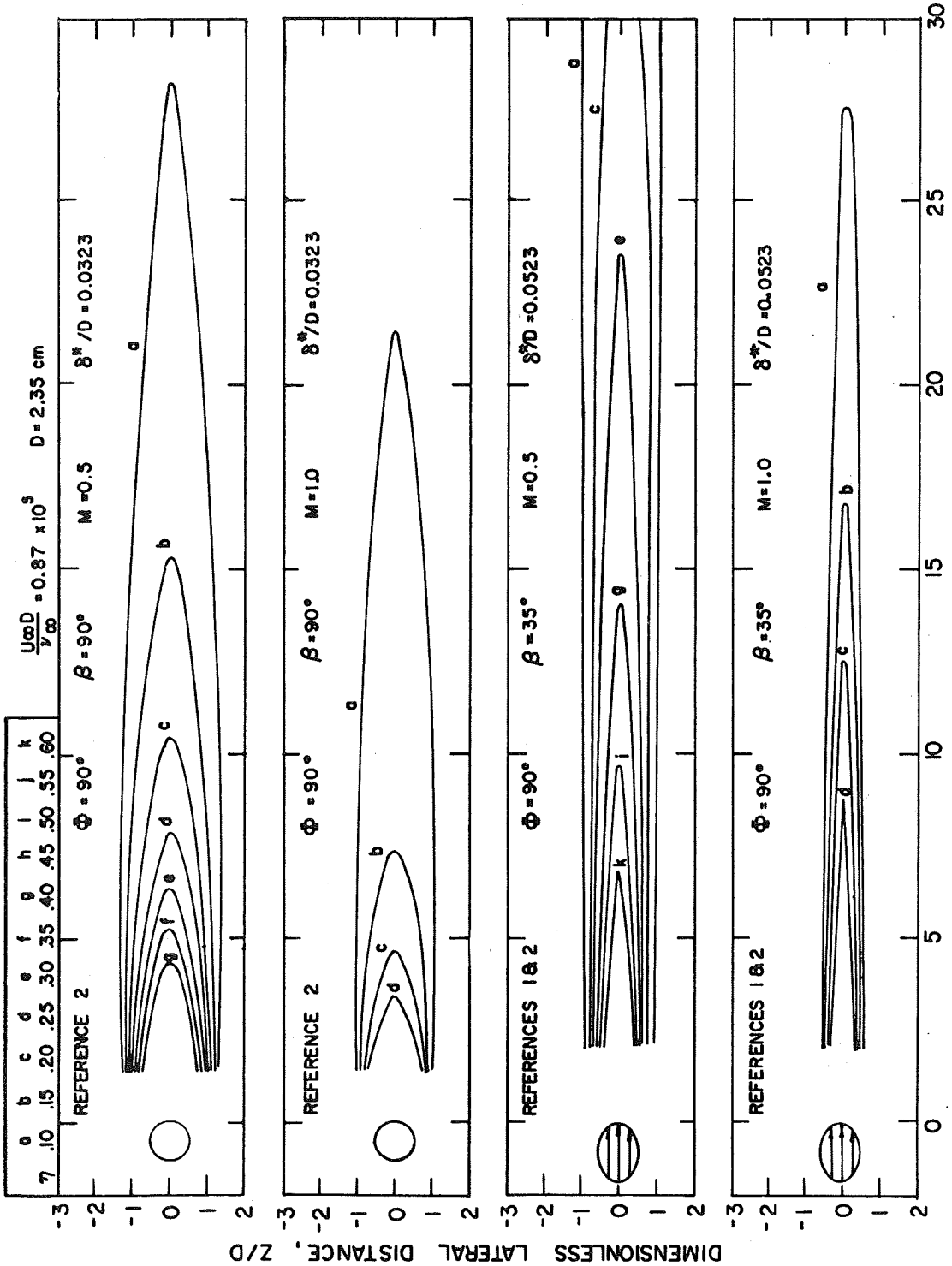

Fig. 27 Lines of constant film cooling effectiveness for normal injection and injection at 35° with the flow

NAS3-7904
SUMMARY REPORT
DISTRIBUTION LIST

ADDRESSEE			NUMBER OF COPIES
1.	NASA Lewis Research Center 21000 Brookpark Road Cleveland, Ohio	Mail Stop	
	Attention: Aeronautics Procurement Section	77-3	1
	Reports Control Office	5-5	1
	Technology Utilization Office	3-19	1
	Library	60-3	2
	Fluid System Components Div.	5-3	1
	I.I. Pinkel	5-3	1
	W. L. Stewart	77-2	1
	J. Howard Childs	60-4	1
	J. B. Esgar	60-4	1
	F. S. Stepka	60-6	10
	R. O. Hickel	60-6	1
	H. Ellerbrock	60-4	6
	L. Macioce	60-6	1
	J. Livengood	60-6	1
2.	NASA Scientific & Technical Information Facility P.O. Box 33 College Park, Maryland 20740 Attention: NASA Representative RQT-2448		6
3.	FAA Headquarters 800 Independence Avenue, S.W. Washington, D.C. 20546 Attention: Robert Pines		1
4.	NASA Headquarters Washington, D.C. 20546 Attention: N. F. Rekos (RAP)		1
5.	Department of the Army U.S. Army Aviation Material Laboratory Fort Eustis, Va. 23604 Attention: John White		1
6.	Headquarters Wright-Patterson AFB, Ohio 45433 Attention: Kenneth Hopkins (AFAPL/APTC)		2

7. Air Force Office of Scientific Research
Propulsion Research Division
USAF Washington, D.C. 20025 — 1

8. Defense Documentation Center (DDC)
Cameron Station
5010 Duke Street
Alexandria, Virginia 22314 — 1

9. NASA-Langley Research Center
Langley Station
Technical Library
Hampton, Virginia 23365
Attention: Mark R. Nichols — 1
John V. Becker — 1

10. United Aircraft Corporation
Pratt & Whitney Aircraft Division
Florida Research & Development Center
P.O. Box 2691
West Palm Beach, Florida 33402
Attention: R. A. Schmidtke — 1

11. United Aircraft Corporation
Pratt & Whitney Aircraft Division
400 Main Street
East Hartford, Connecticut 06108
Attention: C. Andreini — 2
Library — 1

12. United Aircraft Research
East Hartford, Connecticut
Attention: Library — 1

13. Allison Division of GMC
Department 8894, Plant 8
P.O. Box 894
Indianapolis, Indiana 46206
Attention: J. N. Barney — 1
C. E. Holbrook — 1
Library — 1

14. Northern Research & Engineering Corporation
219 Vassar Street
Cambridge, Massachusetts
Attention: K. Ginwala — 1

15. General Electric Company
Flight Propulsion Division
Cincinnati, Ohio 45215

Attention:			
	J. W. McBride	N-44	1
	F. Burggraf	H-32	1
	S. N. Suciu	H-32	1
	Technical Information Center	N-32	1

16. General Electric Company
1000 Western Avenue
West Lynn, Massachusetts 01905
Attention: Dr. C.W. Smith-Library Bldg. 2-40M 1

17. Curtiss-Wright Corporation
Wright Aeronautical Division
Wood-Ridge, New Jersey 07075
Attention: S. Lombardo 1

18. Air Research Manufacturing Company
402 South 36th Street
Phoenix, Arizona 85034
Attention: Robert O. Bullock 1

19. Air Research Manufacturing Company
9851 Sepulveda Boulevard
Los Angeles, California 90009
Attention: Dr. N. Van Le 1
Dr. P. J. Berenson 1

20. AVCO Corporation
Lycoming Division
350 South Main Street
Stratford, Connecticut 06497
Attention: Claus W. Bolton 1
Charles Kuintzle 1

21. Continental Aviation & Engineering Corporation
12700 Kercheval
Detroit, Michigan 48215
Attention: Eli H. Benstein 1
Howard C. Walch 1

22. International Harvester Company
Solar Division - 2200 Pacific Highway
San Diego, California 92112
Attention: P. A. Pitt 1
Mrs. L. Walper 1

23. George Derderian AIR 53662 B
Department of Navy
Bureau of Navy
Washington, D.C. 20360 — 1

24. The Boeing Company
Commercial Airplane Division
P.O. Box 3991
Seattle, Washington 98124
Attention: C. J. Schott — 80-66 — 1

25. Aerojet-General Corporation
Sacramento, California 95809
Attention: M. S. Nylin — 1
Library — 1
Rudy Bear — 1

26. Newark College of Engineering
323 High Street
Newark, New Jersey 07102
Attention: Dr. Peter Hrycak — 1

27. Department of Mechanical Engineering
Arizona State University
Tempe, Arizona
Attention: Dr. D. E. Metzger — 1